skb.se

**SKB P-22-05**

ISSN 1651-4416

ID 1973832

December 2022

# Effects of a warmer climate on near-surface water balances of biosphere objects examined in the post-closure safety assessments for SFR

## Simulations with MIKE SHE SR-PSU 5000 AD model

Mona Sassner, DHI Sverige AB

Johan Liakka, Jean Marc Mayotte
Svensk Kärnbränslehantering AB

*Keywords:* near-surface hydrology, local hydrological model, regional hydrological model, warm climate, water balances, biosphere objects, post-closure safety, SFR, Forsmark

# Abstract

This report presents the results from near-surface hydrological simulations for the preliminary safety analysis report (PSAR) for SFR. These simulations include a warmer climate than at present and are carried out using both a regional and local scale hydrological model. The local model encompasses SFR and the biosphere objects of relevance to the PSAR for SFR: objects 116, 157_1, 157_2 and 159. The landscape characteristics used in the modelling are postulated to be characteristic of the Forsmark landscape after the shoreline has receded from the area (assumed to be 5000 AD). Results from the simulations are presented as maps. These maps show the calculated depth to groundwater and the predicted location of the groundwater recharge and discharge areas at the surface of the model. Results of the simulations performed using the local model are also presented in the form of water balances. Water balances are presented for the entire local model area as well as the individual biosphere objects.

# Sammanfattning

Denna rapport presenterar resultat från ytnära hydrologiska simuleringar för den preliminära säkerhetsanalysrapporten (PSAR) för SFR. Simuleringarna antar ett varmare klimat än idag och utförs med hjälp av både en regional och lokal hydrologisk modell. Den lokala modellen omfattar SFR och de biosfärsobjekt som är relevanta för PSAR för SFR: objekt 116, 157_1, 157_2 och 159. Landskapsegenskaperna som används i modelleringen antas vara karakteristiska för Forsmarkslandskapet efter att strandlinjen dragit sig tillbaka från området (antas ske år 5000 e.Kr). Resultat från de simuleringarna presenteras i form av kartor. Dessa kartor visar det beräknade djupet till grundvattnet samt sannolika platser för grundvattentillförsel och utsläppsområden vid ytan. Resultaten från den lokala modellen presenteras också i form av vattenbalanser för hela det lokala modellområdet och för de enskilda biosfärobjekten.

# Table of Contents

# 1 Introduction

This report contributes to the preliminary safety analysis report (PSAR) for SFR, the repository for short-lived low- and intermediate-level radioactive waste in Forsmark in Östhammar municipality (Figure 1-1).

The Swedish Nuclear Fuel and Waste Management Co., SKB, currently operates SFR to dispose of low- and intermediate-level operational waste produced during operation of the Swedish nuclear power plants (Figure 1-2). SFR is situated 60-130 metres below the Baltic seafloor and comprises four 160-metre-long waste vaults and one waste vault with a 50-metre-high concrete silo for the most radioactive waste. Two parallel kilometre-long access tunnels link the facility to the surface.

In 2014, SKB applied for a permit to extend and continue the operation of SFR (Figure 1-2). The extension consists of six waste vaults with a length of 255–275 metres each, located 120–140 metres below the Baltic seafloor. When the extension is complete, SFR will have room for about 200 000 cubic metres of waste, compared with about 63 000 cubic metres today. Post-closure safety for the extended SFR was analysed as part of the first preliminary safety analysis report (F-PSAR) included in the application. After review of the application by the Swedish Radiation Safety Authority (SSM) under the Act on Nuclear Activities and by a Swedish Land and Environmental Court under the Environmental Code, the Swedish Government approved the application in 2021.

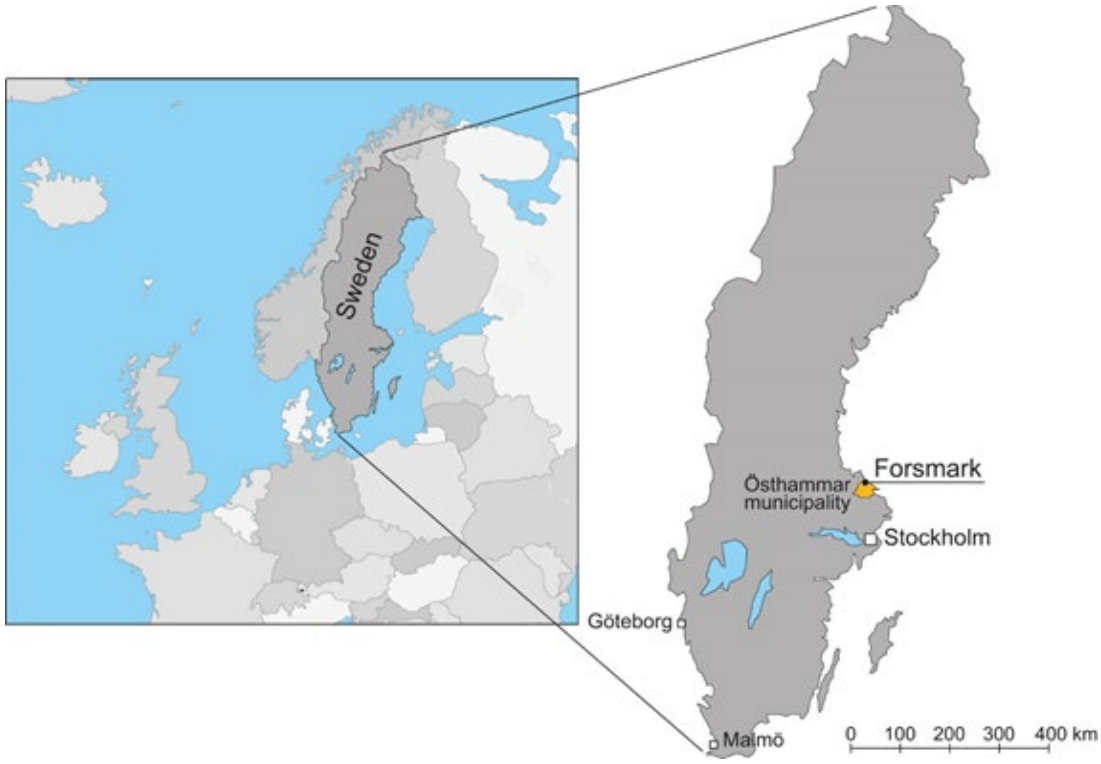


***Figure 1-1.*** *Location of the Forsmark site in Sweden (right) and in context with the countries in Europe (left). The site is situated in the Östhammar municipality, which belongs to the County of Uppsala.*

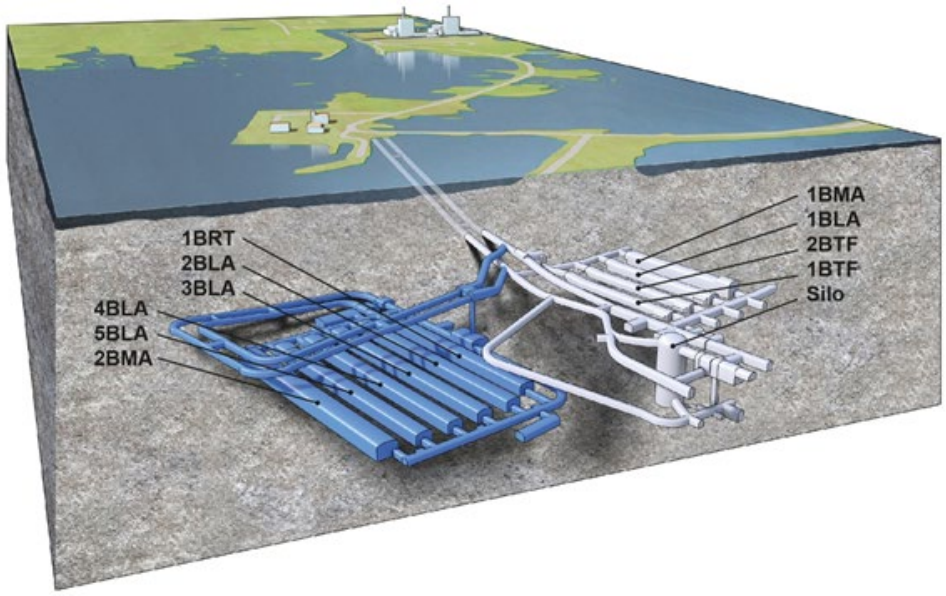


***Figure 1-2.*** *Schematic illustration of SFR. The grey part is the existing repository (SFR1) and the blue part is the planned extension (SFR3). The waste vaults in the figure are the silo for intermediate-level waste, 1–2BMA vaults for intermediate-level waste, 1BRT vault for reactor pressure vessels, 1–2BTF vaults for concrete tanks and 1–5BLA vaults for low-level waste.*

As a part of the license application for the extension of SFR, SKB is continually assessing the long-term radiological safety of the entire future SFR repository (the existing SFR 1 and the planned SFR 3). Hydrological and hydrogeological modelling is an important part of this assessment. Comprehensive analyses of the hydrology and near-surface hydrogeology of the Forsmark area were performed for SR-PSU project using a 3D-numerical model, see Werner et al. (2013). This modelling was based on two sets of climate data: one set representing present-day climate and another set representing a slightly warmer climate with much higher precipitation than at present.

The climate evolutions used in the post-closure safety assessment has been updated for the PSAR. This includes an updated description of a warmer climate based on the most recent scientific literature (SKB TR-23-05, Chapter 3). The climate used in the SR-PSU hydrological simulations (Werner et al. 2013) are not consistent with the updated warm climate for the PSAR. Specifically, the updated climate is significantly warmer and precipitation amounts are lower than assumed in Werner et al. (2013). This report examines the effect of this warmer climate on the hydrology at Forsmark. Results from these hydrological simulations are used in the PSAR for SFR. Apart from the climate, the parameterisation and boundary conditions of the hydrological model used in this report are the same as the 5000 AD model used in Werner et al. (2013). Thus, the future shoreline and landscape configuration for Forsmark at 5000 AD, as described by Brydsten and Strömgren (2013), are assumed.

Modelling results are presented for both the regional and local model area (Figure 2-3) as well as for the individual biosphere objects within the local model area (Figure 2-5). Results are presented in the form of water-balances, i.e., 1D representations of water fluxes within the spatial delineations specific to the regional and local model areas. Water balances for the individual biosphere objects are presented according to the vertical discretization of the soil stratigraphy used in MIKE SHE (see Section 2.2.2). Modelling results are also presented in depth-to-groundwater maps for the regional and local model area.

# 2 Methods

## 2.1 Modelling tool – MIKE SHE

### 2.1.1 Water movement

MIKE SHE is an integrated hydrological model system that describes the main processes in the hydrological cycle on land, including the interaction with the atmosphere in terms of precipitation and evapotranspiration. In the hydrological cycle, water evaporates from the oceans, lakes and rivers, from the soil and is transpired by plants. This water vapour is transported in the atmosphere and falls back to the earth as rain and snow. It infiltrates to the groundwater and discharges to streams and rivers as baseflow. It also runs off directly to streams and rivers that flow back to the ocean. The hydrologic cycle is a closed loop and our interventions do not remove water; rather they affect the movement and transfer of water within the hydrologic cycle. MIKE SHE has been used in several studies initiated by SKB (e.g., Werner et al. 2013, Berglund et al. 2013, Bosson et al. 2012, Jutebring Sterte et al. 2018, 2021).

The MIKE SHE model distribution version used int this study is 2020. A detailed description may be found in DHI (2020) and in Graham and Butts (2005). Figure 2-1 illustrates the different model components in MIKE SHE. The parameterization, boundary conditions and spatial boundaries of the MIKE SHE hydrological model used in this study are the same as that used in SR-PSU project, with the only difference between the models being the climate data used in the simulations. See Werner et al. (2013) for a full description of the processes accounted for in the model.

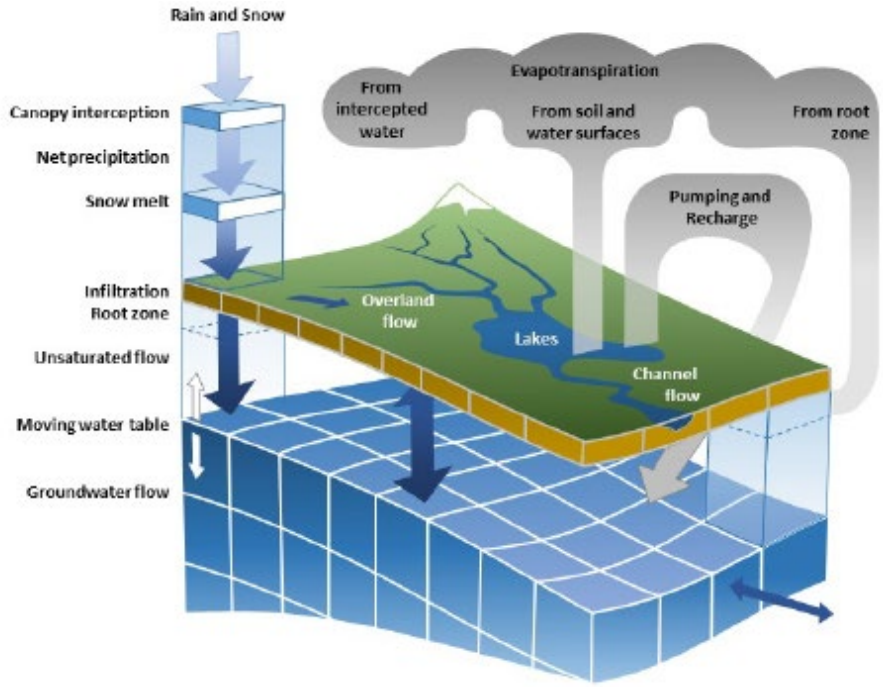


***Figure 2-1.*** *Overview of the MIKE SHE modelling tool and its main components*

### 2.1.2 Water balances

Results of the MIKE SHE model are primarily presented in the form of water balances in this study. The water balance utility in MIKE SHE is a post-processing tool for generating water balance summaries from model simulations. Water balance output can include area-normalized flows (storage depths), storage changes, and model errors for individual model components (e.g., unsaturated zone, evapotranspiration, etc.).

A water balance can be generated at a variety of spatial and temporal scales and in a number of different formats. The water balance can be calculated based on the entire model domain or in just a part of the domain. If the water balance is based on an area resolution, then the water balance will be a summary water balance for either the entire catchment or the sub-areas defined. It is also possible to generate maps of the water balance.

Detailed water balances may be extracted for each of the MIKE SHE model components:

- Snow/precipitation
- Canopy (interception)
- Ponded water (overland)
- Unsaturated zone
- Saturated zone

Figure 2-2 illustrates the main water balance flows examined in the present study.

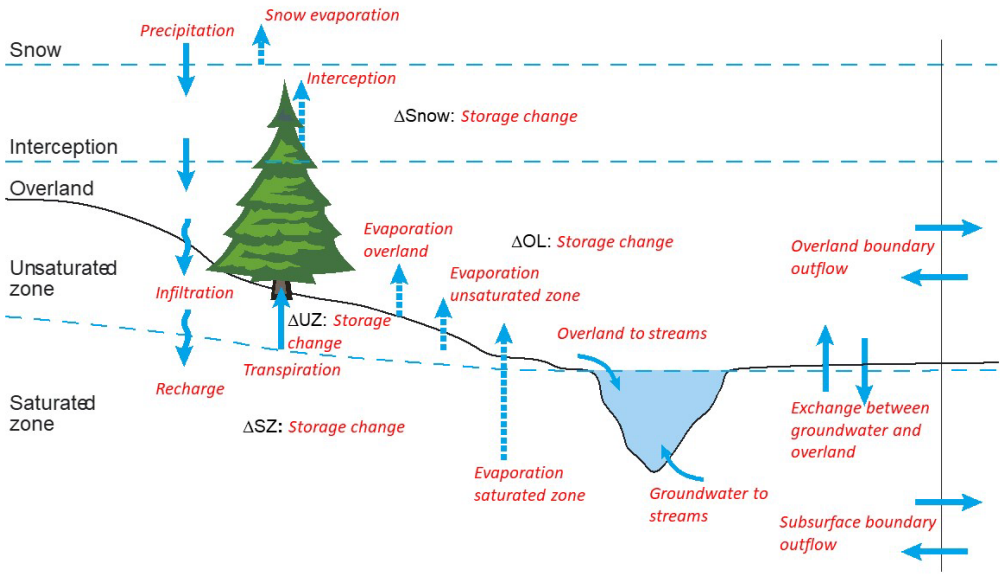


***Figure 2-2.*** *Explanation of main posts in the water balance. The horizontal dashed lines separate the model components.*

## 2.2 Model setup

A full description of the modelling processes and model parameterization of the MIKE SHE model used in the present study is reported in Werner et al. (2013). The spatial setup of the model consists of a regional and a local model area, see Figure 2-3.

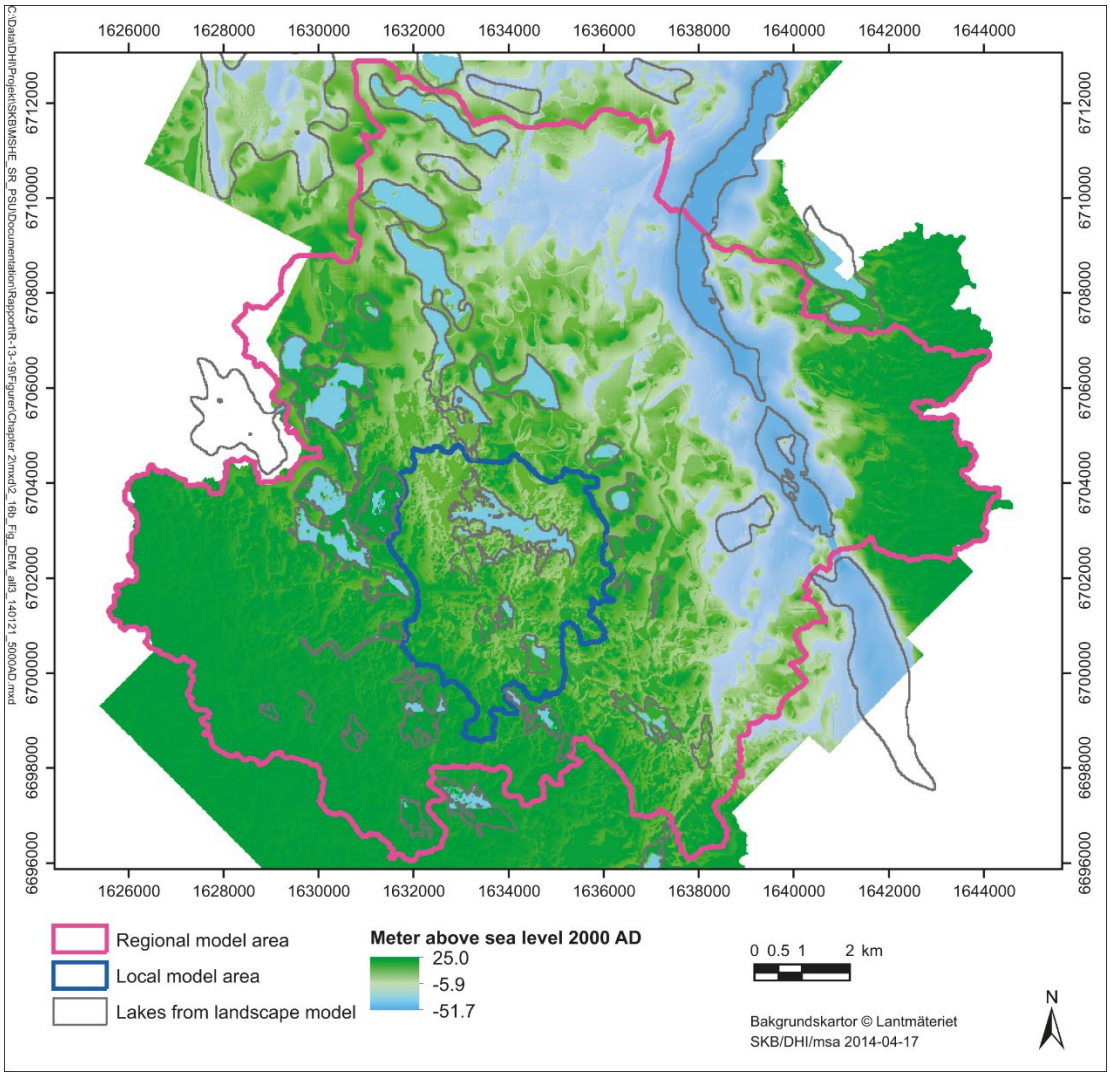


***Figure 2-3.*** *Map showing the regional and local model areas, with a coastline corresponding to 5000 AD (from Werner et al. 2013)*

### 2.2.1 Regional model

The MIKE SHE regional model domain has an area of about 180 km$^2$ and a vertical extent down to a depth of 634 m and the model boundaries follow water divides according to Brydsten and Strömgren (2013). In the horizontal direction, the model resolution is 80 m. In the vertical direction, the grid size varies with depth. The regolith, which is based on the regolith depth and stratigraphy model presented by Brydsten and Strömgren (2013), is divided into two calculation layers and the bedrock is divided into a total of 14 layers, with thinner layers closer to the surface and thicker layers close to the bottom boundary.

In Werner et al. (2013), MIKE SHE models were established to represent hydrological and near-surface hydrogeological conditions at the future times 3000, 5000 and 11 000 AD. The model used in this study is the one representing 5000 AD. The year 5000 AD represents an intermediate stage, with co-existing lakes and mires within the regional MIKE SHE model area.

### 2.2.2 Local model

The local model area is located within the regional model area and at the year 5000 AD the shoreline will be located outside of the local model area (Figure 2-3). The shoreline displacement is primarily caused by isostatic rebound (Brydsten and Strömgren 2010). Thus, the anticipated effects of future sea-level rise in a warmer climate are neglected in this study. The local model is established and used to generate modelling results, whereas the objective of the regional model primarily is to obtain time-varying external boundary conditions for the local model.

The horizontal resolution of the local model is 20 m. In the vertical direction in local model, the regolith model presented by Brydsten and Strömgren (2013) is divided into 4 calculation layers. Moreover, down to a depth of about 90 m, each calculation layer in the bedrock of the regional model is in the local models divided into two calculation layers, which results in 23 calculation layers in the rock. Figure 2-4 illustrates the differences between the numerical vertical discretization for the regional (left side) and the local (right side) models, for the upper 150 m.

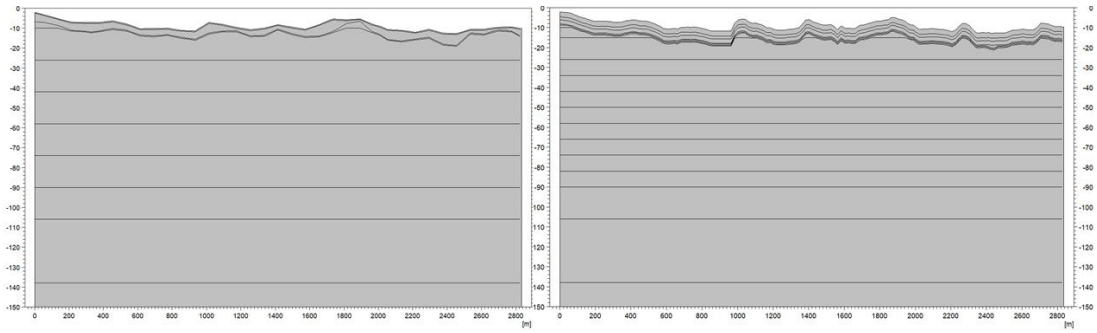

***Figure 2-4.*** *Example profile showing the vertical resolution in the regional (left) and local (right) models for the upper 150 m*

## 2.3 Biosphere objects

In the SR-PSU project, seven biosphere objects were identified based on discharge locations at the interface between rock and regolith, calculated using forward particle tracking in DarcyTools, see Werner et al. (2013). Water balance results for the biosphere objects from MIKE SHE are used to generate model inputs to the radionuclide transport model. The methodology used to translate the MIKE SHE water balance results to the discretization used in the radionuclide transport model is presented in Chapter 7 in Werner et al. (2013) and in Sassner (2022).

The biosphere objects marked Figure 2-5 are used in the present study. In 5000AD, three of the objects (157_1, 159 and 116) are estimated to be lake areas with surrounding mire areas, while object 157_2 is estimated to consist of only a mire. In the model water is discharged downstream from object 157_2 to 157_1, primarily via overland flow. Water from object 159 is transported downstream to object 157_1 via a stream. The largest object, 116, will receive water from all three upstream objects (i.e. 157_2, 159 and 157_1).

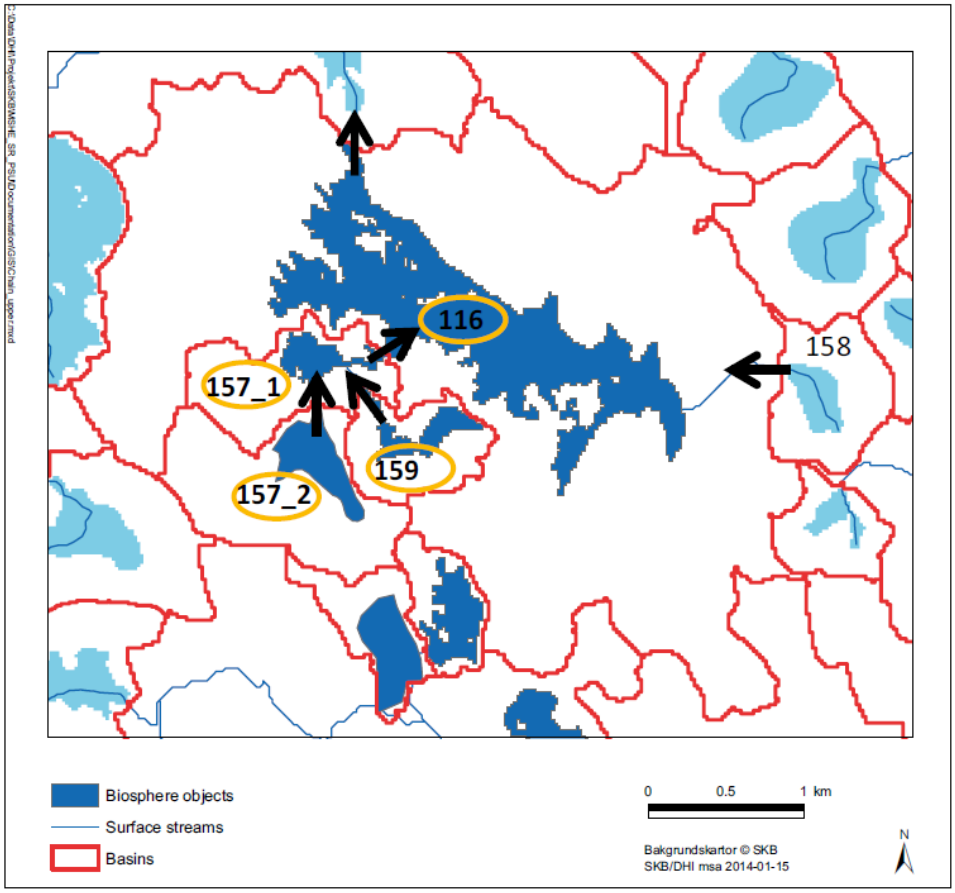


***Figure 2-5.*** *Biosphere objects for which water balances are presented in this study marked with a yellow circle.*

MIKE SHE water balance results are extracted and processed prior to being input into the radionuclide transport model. For the regional model area, outputs from the MIKE SHE model are delivered in the format presented in Figure 2-2. Explanation of main posts in the water balance. The horizontal dashed lines separate the model components. Figure 2-6 and Figure 2-7 show the format with which the extracted flows are presented for each biosphere object. Figure 2-7 shows the specific water balance results extracted for a lake-mire-area. Figure 2-7 specifies the water balance items for an area with only a mire. See Chapter 7 in Werner et al. (2013) for a more detailed description of how the water balances are applied to the BioTEx model.

The regolith description in the MIKE SHE models is based on the model for regolith depth and stratigraphy presented by Brydsten and Strömgren (2013). In the local model, the total regolith depth is divided into 4 calculation layers, named Rego1 to Rego4 in Figure 2-6 and Figure 2-7. The uppermost calculation layer in MIKE SHE, Rego1, has a thickness of 2.5 m in order to allow proper calculations of evapotranspiration processes (for more details, see Bosson et al. 2008).

In the delivery to the radionuclide-transport modelling, Rego1 was divided into two layers, with thicknesses of 0.5 m (Rego1a) and 2.0 m (Rego1b). Specifically, near-surface groundwater flow is assigned to Rego1a, whereas other contributions are distributed according to relative thickness (20% to Rego1a and 80% to Rego1b). Accordingly, vertical groundwater flows are recalculated to obtain layer-wise water balances based on these distributions of horizontal flows. For more details, see Werner et al. (2013).

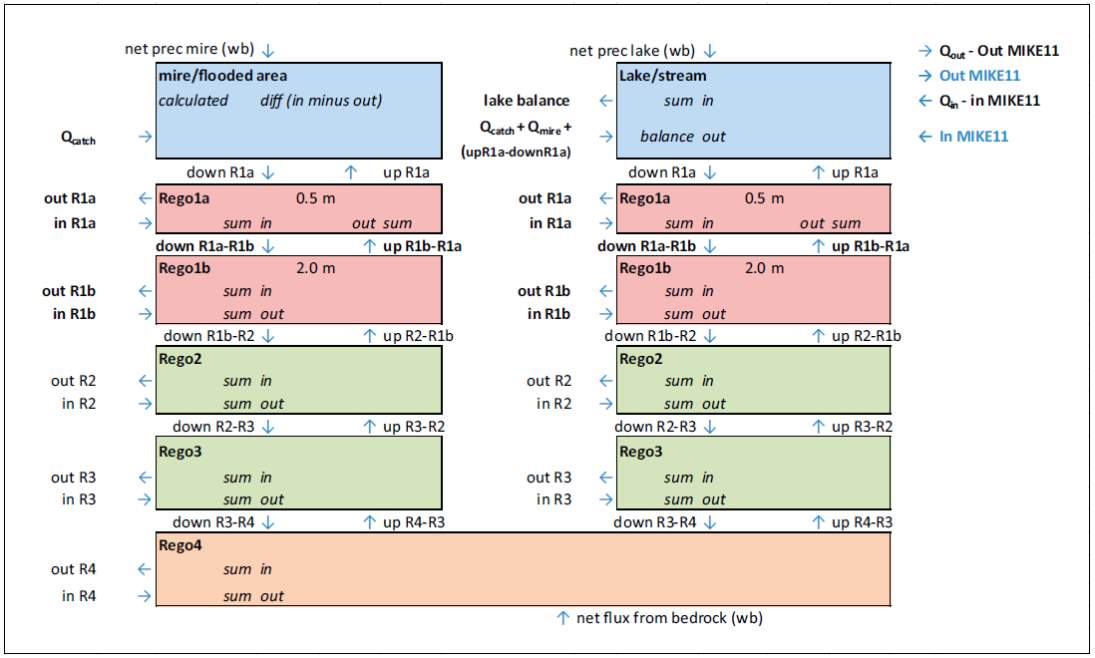


***Figure 2-6.*** *Box model for water balances for biosphere objects with both mire and lake areas and with a surface stream.*

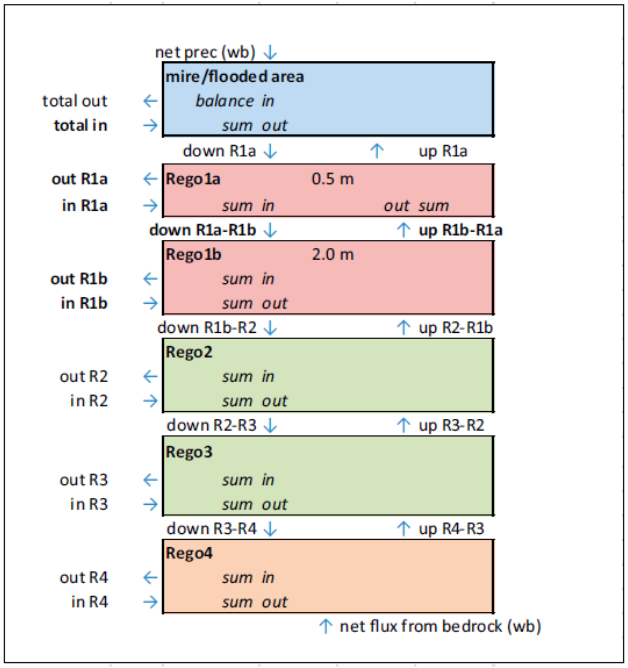


***Figure 2-7.*** *Box model for water balances for object with only mire areas.*

# 3 Climate data

## 3.1 Introduction

As previously mentioned, the climate data used for the analyses presented herein are meant to compliment the climate cases examined in hydrological modelling conducted in Werner et al. (2013). A brief explanation of the climate cases used for the modelling conducted in Werner et al. (2013) is presented immediately below. See Section 2.2 in Werner et al. (2013) for a more in-depth explanation of the climate cases used in the hydrological modelling conducted during SR-PSU.

Two temperate climate cases were examined in the hydrological modelling presented in Werner et al. (2013): present-day climate and a possible wetter and warmer future climate. The present-day climate case was represented by locally measured meteorological data during a selected 1-year period between October 1, 2003 and September 30, 2004. This selected one-year period, referred to as the *normal year*, had an annual average air temperature of 6.4 °C (minimum –13.2 °C and maximum 23.4 °C) and an accumulated precipitation of 583 mm.

The wetter and warmer climate case was also constructed using data from measurements and climate model simulations. This climate case had an average air temperature of 7.7 °C (minimum –16.1 °C and maximum 24.2 °C) and an annual average precipitation of 1500 mm.

The climate evolutions used in the post-closure safety assessment has been updated for the PSAR. This includes an updated description of a warmer climate based on the most recent scientific literature (SKB TR-23-05, Chapter 3). Specifically, the reference evolution of the present assessment includes the *warm climate variant* (SKB TR-23-01, Chapter 6), which accounts for up to 5 °C warming relative to present day. Below follows a brief description of the updated air temperature at 5000 AD that is consistent with the warming described in the *warm climate variant* (Section 3.2). This representation of the air temperature is subsequently used as input in the calculations of precipitation (Section 3.3) and potential evapotranspiration (Section 3.4).

## 3.2 Air temperature and precipitation

The air temperature input data, representative for a warmer climate, are governed by the following equation:

$$T = T_{baseline} + \Delta T. \qquad \text{Equation 3-1}$$

$T_{baseline}$ represents the normal-year daily-averaged air temperature (see above), and $\Delta T$ the global warming-induced change in Forsmark air temperature over the coming 10 000 years. The methodology to construct the temporal evolution of $\Delta T$ is described in detail in SKB (TR-23-05, Appendix B1). In short, the temporal evolution of $\Delta T$ is based on results from several global climate models, including those from the Intergovernmental Panel on Climate Change (IPCC) fifth assessment report (IPCC 2013) and models that cover longer timescales (up to 10 000 years) than the IPCC. Furthermore, the construction of $\Delta T$ accounts for seasonal differences in the warming, i.e. that a warming typically is expected to be more pronounced during winter than during summer.

$\Delta T$ is constructed for three Representative Concentration Pathways (RCP) emissions scenarios from IPCC (2013): RCP8.5 (Figure 3-1). Aside from future greenhouse-gas emissions, the uncertainty in future climate warming primarily stems from an incomplete understanding of the climate system, resulting in poorly constrained parameterisations of these processes in the models that project the future climate. This uncertainty is often expressed in terms of varying *climate sensitivity*, defined as the equilibrium global air temperature increase in response to a doubling of the atmospheric $CO_2$ concentration[1]. To account for the uncertainty related to the climate sensitivity, three evolutions of $\Delta T$ are provided for each RCP; a "best-estimate" average

[1] According to IPCC (2013), climate sensitivity is likely in the range from 1.5°C to 4.5°C per doubling of atmospheric $CO_2$ (IPCC 2013).

evolution, corresponding to mid-range climate sensitivity, as well as two bounding cases of $\Delta T$, corresponding to low and high climate sensitivity, respectively (Figure 3-1).

The maximum warming in the *warm climate variant* amounts to 5 °C above the present-day air temperature. This warming is also considered in the parameterisations of the radionuclide transport and dose models employed to evaluate radiological consequences of a warmer climate on post-closure safety. At 5000 AD, $\Delta T$ arising from the lower bound of RCP8.5 is very similar the maximum warming of the *warm climate variant*, and is therefore used to describe the warmer climate in the hydrological simulations. The mean annual increase of $\Delta T$ for this development is 5.0 °C, and the increase is slightly higher during the winter season than during summer (Table 3-1). The resulting air temperatures over a year are obtained by adding the anomalies in Table 3-1 to the normal-year air temperatures ($T_{baseline}$). These air temperatures are shown in Figure 3-2.

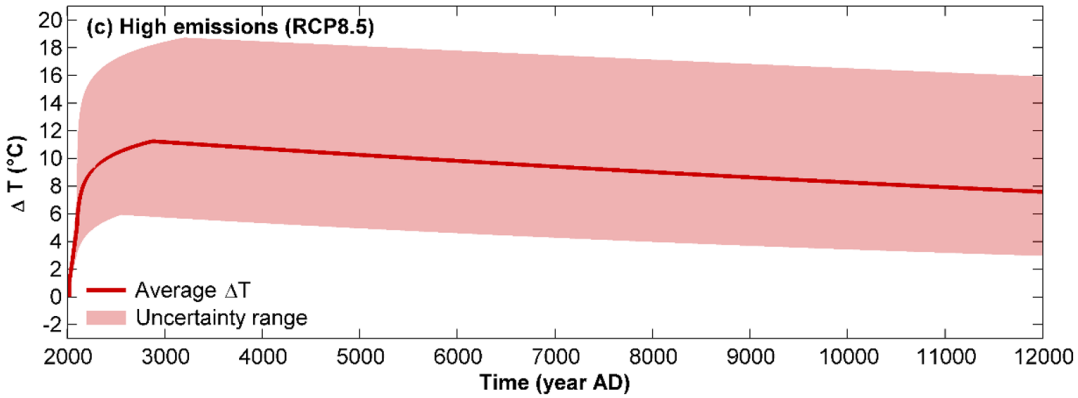


***Figure 3-1.*** *Constructed annual mean surface air temperature change (**ΔT**) until 12 000 AD at Forsmark (relative to present) for future anthropogenic greenhouse-gas emissions consistent with the RCP8.5 scenarios (IPCC 2013). Shading indicates the total uncertainty of **ΔT** and the solid lines indicate the average "best-estimate" ΔT for each RCP. For more information on how **ΔT** is computed, see SKB (TR-23-05, Appendix B1).*

**Table 3-1. Seasonal characteristics of $\Delta T$ corresponding to the lower bound of RCP8.5 at 5000 AD.**

| Season | $\Delta T$ |
|---|---|
| December – February | 5.9 |
| March – May | 5.0 |
| June – August | 4.2 |
| September – November | 4.7 |

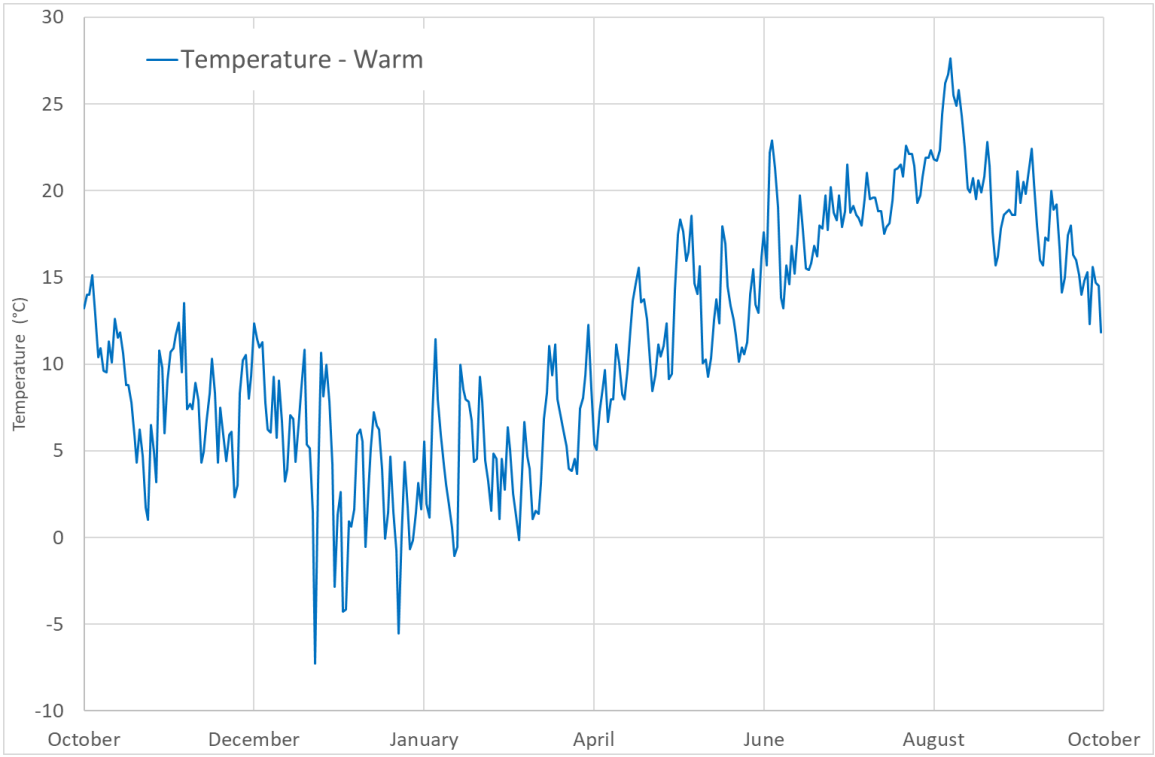


***Figure 3-2.*** *Daily mean temperature in a warmer climate, used as input to calculation of precipitation (Section 3.3) and potential evapotranspiration (Section 3.4).*

## 3.3 Precipitation

The precipitation in a warmer climate is parameterised according to the following equation:

$$P = P_{baseline} \times \Delta P, \qquad \text{Equation 3-2}$$

where $P_{baseline}$ represents the normal-year daily precipitation (Section 3.1), whereas $\Delta P$ represents the relative change in precipitation due to a warmer climate[2]. Climate model projections indicate that the fractional change in precipitation, on a seasonal basis, is roughly proportional to the change in air temperature (SKB TR-23-05, Appendix B2). Thus, the following relationship is approximately true:

$$\Delta P = 1 + \varphi \Delta T, \qquad \text{Equation 3-3}$$

where $\varphi$ (unit °C$^{-1}$) is the rate of relative precipitation change per unit of absolute air temperature change. The value of $\varphi$ is determined by examining global warming projections from seven global climate models and one regional climate model (SKB TR-23-05, Appendix B2). All of the examined models suggest that precipitation in the Forsmark region increases as a result of a climate warming during the winter, spring and autumn seasons. Based on the model projections $\varphi$ is set to 0.04 °C$^{-1}$ for these seasons. For the summer season, however, the precipitation response is much more divergent across the models. Whilst three out of the seven global models project a significant increase of the summer precipitation, the remaining four models suggest either a significant summer precipitation decrease or a limited precipitation change relative to present day. Therefore, $\Delta P$ is provided in two variants for the summer season; either with increased ($\varphi = 0.04$ °C$^{-1}$) or decreased ($\varphi = -0.03$ °C$^{-1}$) summer precipitation relative to present day, respectively. Further details about the choice of $\varphi$ is given in SKB (TR-23-05, Appendix B2). The resulting cumulative precipitation over a year in the two variants is shown in Figure 3-3.

[2] In contrast to the air temperature, precipitation cannot be less to zero. Therefore, changes in precipitation are expressed as ratios rather than differences.

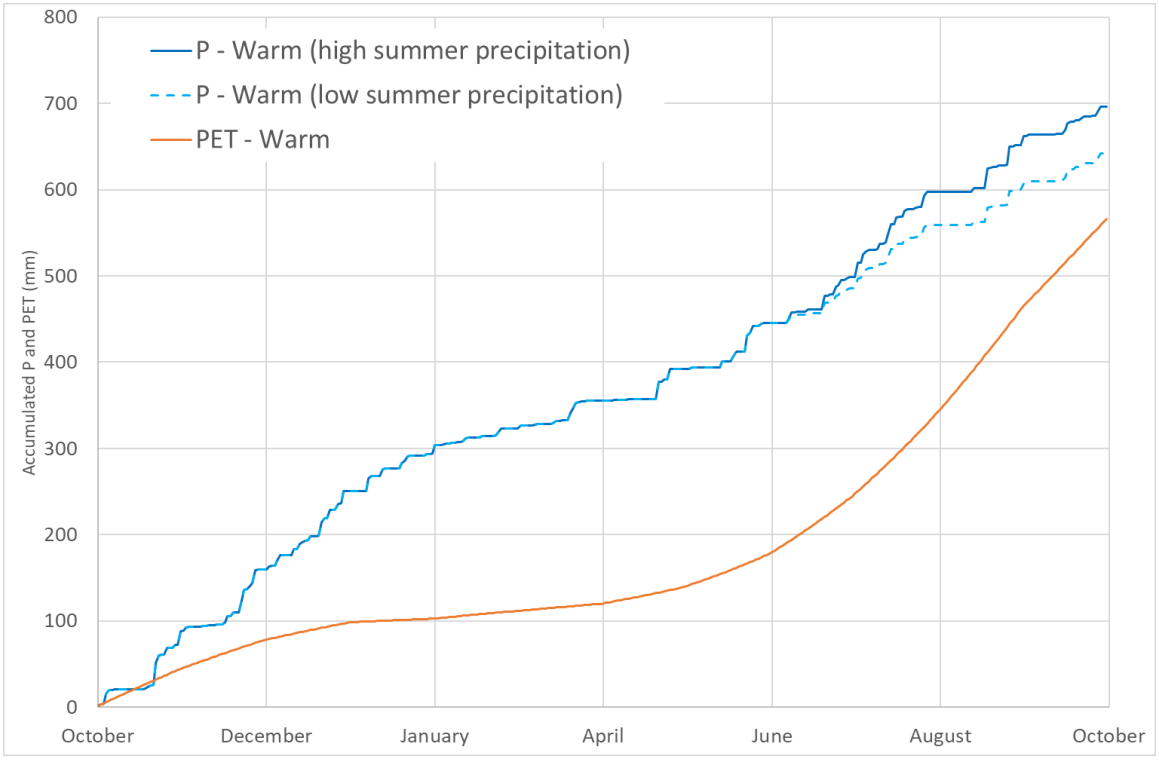


***Figure 3-3.*** *Cumulative precipitation and potential evapotranspiration over a year. These data are used as input for the hydrological modelling in MIKE-SHE.*

## 3.4 Potential evapotranspiration (PET)

The chosen methodology for estimating PET changes in a warmer climate is adopted from Pereira and Pruitt (2004). It combines the Thornthwaite equation (Thornthwaite 1948) with the Willmott equation (Willmott et al. 1985) to calculate the daily PET using air temperature and day-length as input. Day length is defined as the time between sunrise and sunset, and thus varies considerably at Forsmark during a year. In addition to those sub-annual variations, however, day length also changes slowly over timescales associated with Earth's orbital variants which can be predicted with high accuracy for the next 100 ka and beyond (e.g. Berger 1978)[3]. Further details on the chosen PET methodology is given in SKB (TR-23-05, Appendix E).

The cumulative PET over a year is shown in Figure 3-3. It is calculated using the air temperatures in Figure 3-2. Furthermore, in the calibration of the site-descriptive model of Forsmark, PET was reduced by 15 % to the original data (Bosson et al. 2008). To ensure a consistent handling across models, the same reduction of PET is also applied to the data in this study.

[3] Specifically, day-length at a certain latitude is computed from the solar declination angle, see e.g. Roderick (1992).

# 4 Results on model area scale

The purpose of the hydrological modelling is to estimate how the hydrology at Forsmark would look under the warmer climate conditions presented in Chapter 3 above. The hydrological modelling is done by "looping" the one-year time-series climate data over the course of the simulation time until inter-annual variabilities in water storages are small. This is done in order to reduce the effects of hysteresis (i.e. the effects of historical conditions) on model results. This means that inter-annual variabilities in the projected climate are ignored by the model and results should be viewed as conditions representative of a "typical" hydrological year (i.e. Oct 1st to Sep 30th) under these climatic conditions.

## 4.1 Regional model

The regional model was run for a period of 8 years for the two climate scenarios presented in Chapter 3. Figure 4-1 shows the area for which the water balances were extracted from the regional model. The red area is the sea at 5000 AD and thus the green areas are land. However, in order to avoid sea water in the water balances during periods with high sea water levels, a buffer area is set between the water balance area and the sea which is not used in the calculation of the water balances.

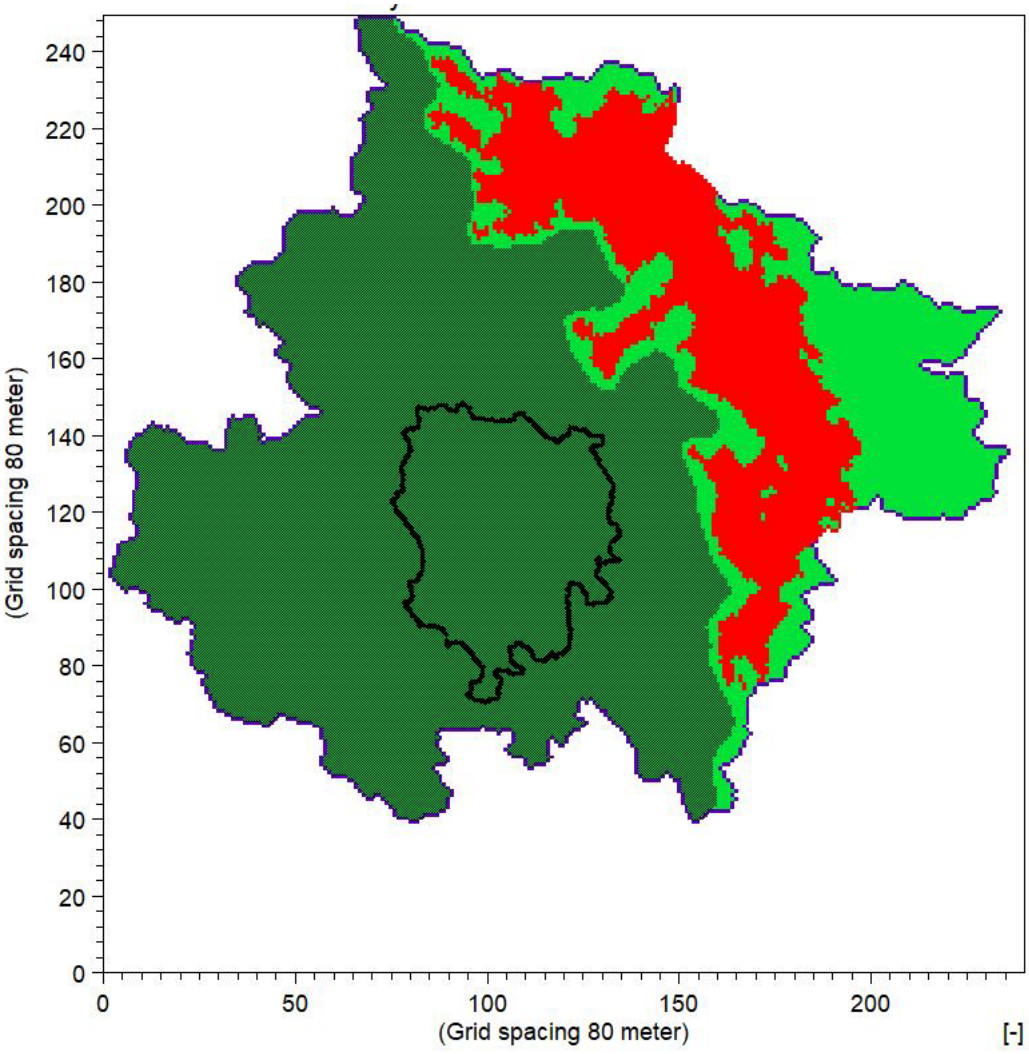


***Figure 4-1.*** *Area for which water balances for the regional model were extracted (dark green). The red area is the extent of the sea at 5000 AD. The light-green area represents a "buffer zone" around the sea. The black line illustrates the boundary of the local model area.*

Table 4-1 and Table 4-2 show the annual values for the main water balance components of the regional model for the warm climate with high (Table 4-1) and low (Table 4-2) summer precipitation datasets. Results are presented for each of the eight years the models were run. Minor differences in the yearly precipitation used by the model (~1 mm/yr) were observed throughout the simulations due to the adaptive time-stepping procedures used in MIKE SHE. These changes are not presented.

**Table 4-1. Main water balance components of the regional model for each simulated year for the warm climate scenario with high summer precipitation. The notation "ΔS" means "change in storage". The error column indicates discrepancies in the water balance. All values are presented in mm/year.**

| Simulation Year | Evapo-transpiration | ΔS Canopy[a] | ΔS Overland[b] | ΔS Sub-surface[c] | Change in net flows to surface water | Change in net boundary outflow | Error |
|---|---|---|---|---|---|---|---|
| 1 | 445 | 0.00 | 72.8 | -12.8 | - | - | 35.4 |
| 2 | 439 | 0.00 | 8.7 | 10.7 | 17.4 | 6.8 | 13.9 |
| 3 | 439 | 0.00 | 2.4 | -0.8 | 6.8 | 0.2 | 3 |
| 4 | 440 | 0.00 | 0.6 | -0.4 | 1.7 | -0.1 | 3.3 |
| 5 | 439 | 0.00 | 0.3 | -0.2 | 0.3 | -0.1 | 3.4 |
| 6 | 439 | 0.04 | 0.5 | 0.6 | -0.4 | 0 | 3 |
| 7 | 439 | 0.00 | -0.1 | -0.1 | 0.4 | -0.1 | 2.7 |
| 8 | 439 | 0.00 | 0.2 | 0 | 0.1 | 0.1 | 3.3 |

[a]: also known as "interception" in the model nomenclature
[b]: "surface" water in rivers and lakes. Also known as "ponded" water in the model nomenclature
[c]: includes water in both the saturated and unsaturated zone

**Table 4-2. Main model water balance items for each calculated year for the warm climate scenario with low summer precipitation. All numbers are presented in mm/year.**

| Simulation Year | Evapo-transpiration | ΔS Canopy[a] | ΔS Overland[b] | ΔS Sub-surface[c] | Change in net flows to surface water | Change in net boundary outflow | Error |
|---|---|---|---|---|---|---|---|
| 1 | 425 | 0.00 | 69.7 | 69.7 | - | - | 42.9 |
| 2 | 418 | 0.00 | 8.5 | 8.5 | 2.6 | 4.5 | 14.8 |
| 3 | 418 | 0.00 | 2.5 | 2.5 | 7.3 | 0.3 | 4.2 |
| 4 | 418 | 0.00 | 0.9 | 0.9 | 0.8 | -0.2 | 3.8 |
| 5 | 418 | 0.00 | 0.2 | 0.2 | 0.2 | -0.1 | 3.7 |
| 6 | 417 | 0.04 | 0.4 | 0.4 | -0.1 | 0.0 | 3.4 |
| 7 | 418 | 0.00 | 0.1 | 0.1 | 0.4 | -0.1 | 3.2 |
| 8 | 418 | 0.00 | 0.0 | 0.0 | -0.1 | 0.1 | 3.4 |

[a]: also known as "interception" in the model nomenclature
[b]: "surface" water in rivers and lakes. Also known as "ponded" water in the model nomenclature
[c]: includes water in both the saturated and unsaturated zone

The error of the model simulations (rightmost column in Table 4-1 and Table 4-2) are the sum of all the discrepancies in the water balance for all of the different model compartments (i.e. snow, canopy, overland, unsaturated, and saturated zone). A positive error implies that the model is generating water, while a negative error means that the model is losing water. For the first year of

each simulation the total error is relatively high for both climate scenarios (about 35-43 mm/year) but then decreases rapidly to 3–4 mm/year by the third year of simulation for both climate scenarios. An error of 3–4 mm/yr is considered acceptable since it is only about 0.5 % of the annual precipitation.

Figure 4-2 and Figure 4-3 show the change in storage over time for the overland model compartments (upper panels) and the subsurface model compartments (lower panels) for the regional model simulated using the warm climate with high (Figure 4-2) and low (Figure 4-3) summer precipitation datasets. Results from both scenarios indicate that the differences in the main water balance items are small (Table 4-1 and 4-2), and seasonal patterns have stabilized (Figure 4-2 and 4-3) after 3–4 years of simulation. It was therefore considered reasonable to use the last 5 years of each simulation as time-varying boundary conditions for their respective local models (see next section).

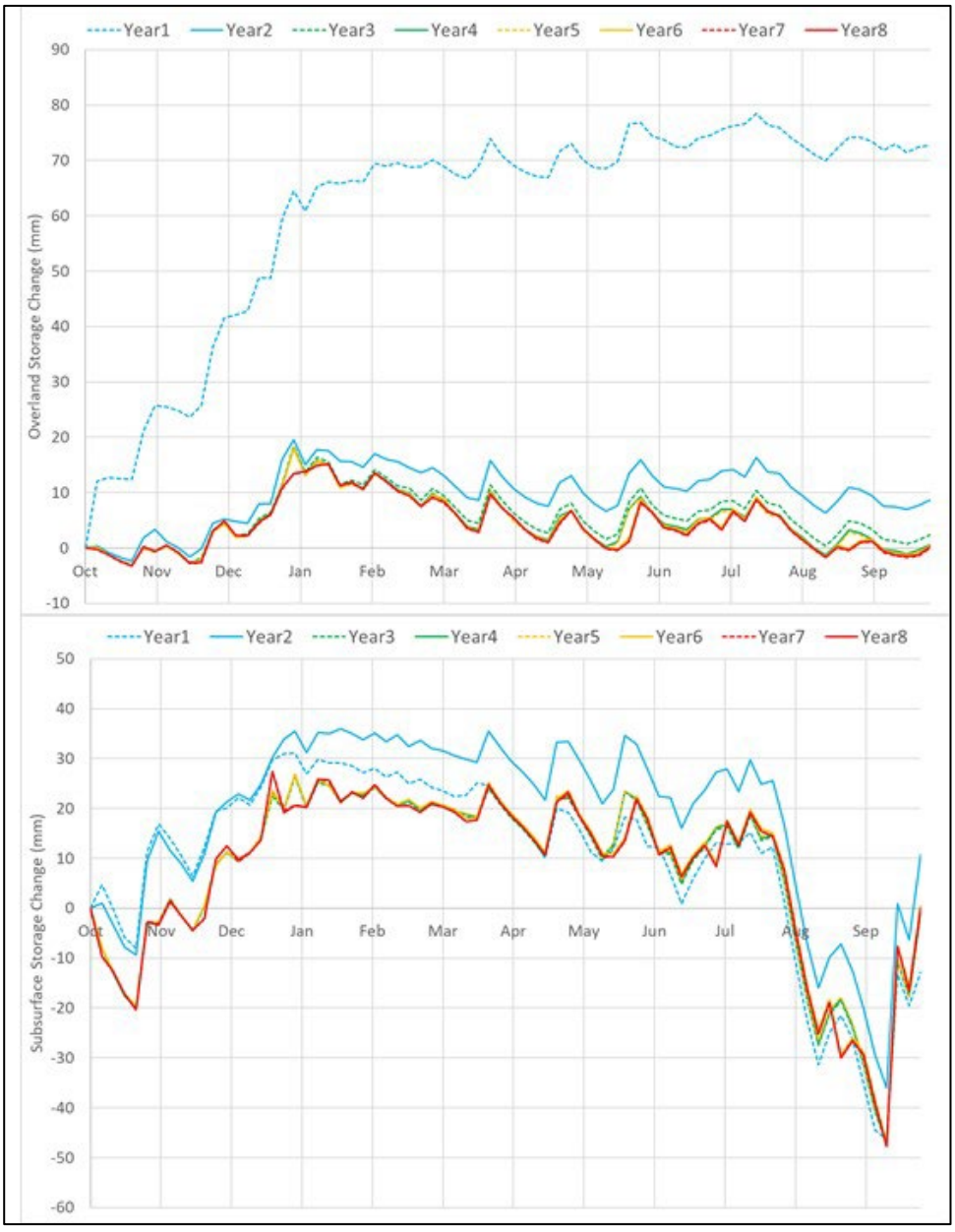


***Figure 4-2.*** *Change of storages (in mm) for both overland storage change (upper figure) and subsurface storage change (lower figure) for the warm climate scenario with a high summer precipitation. Each line in the figures represent a year of simulation.*


***Figure 4-3.*** *Change of storages for both surface (upper figure) and subsurface (lower figure) for the warm climate scenario with a low summer precipitation. Each line in the figures represent a year of simulation.*

Figure 4-4 and Figure 4-5 show the depth to the phreatic water surface[4] for the regional model simulated using the warm climate with high (Figure 4-4) and low (Figure 4-5) summer precipitation datasets. Both figures show simulated, monthly average data for August in the last year of the model simulation. August was chosen as it is the "driest" month according to the climate data used for in the simulation, i.e. August has the highest average temperature (Figure 3-2), low precipitation (Figure 3-3), and high evapotranspiration (Figure 3-3).

[4] The phreatic surface indicates the location where the pore water pressure is under atmospheric conditions (i.e. the pressure head is zero). This surface normally coincides with the groundwater table.

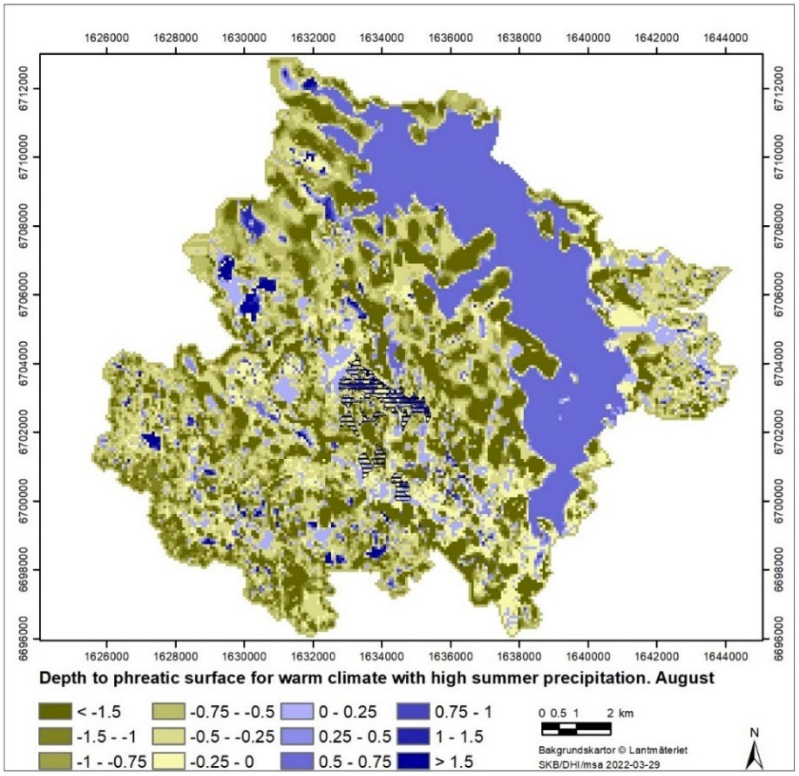


***Figure 4-4.*** *Depth to the phreatic surface for the regional model during a summer period (August) in the last year of calculation for the warm climate with a high summer precipitation. Positive values (blue areas) means that there is water on the surface.*

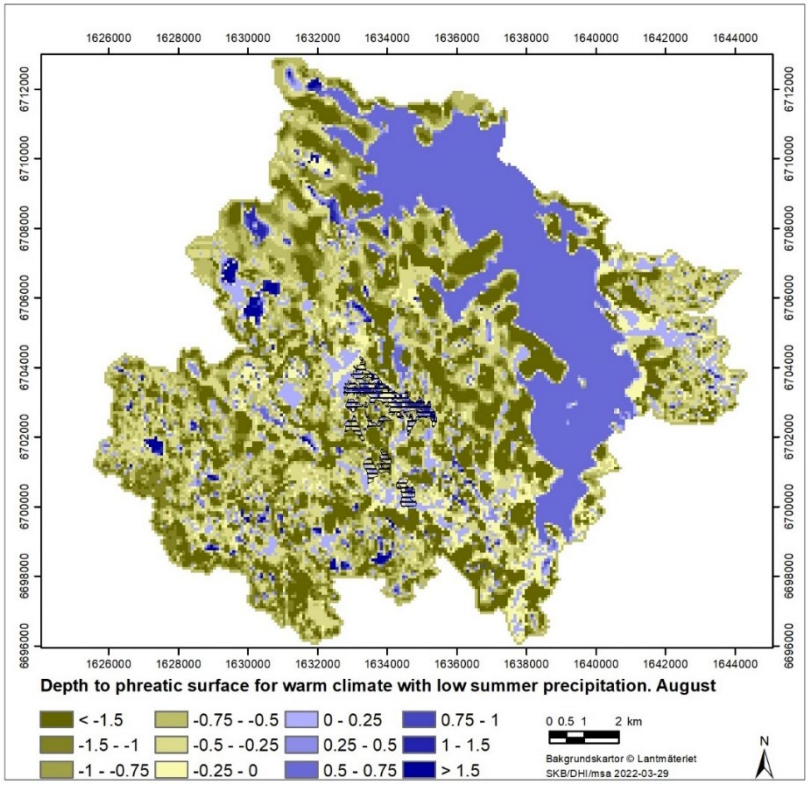


***Figure 4-5.*** *Depth to the phreatic surface for the regional model during a summer period (August) in the last year of calculation for the warm climate with a low summer precipitation. Positive values (blue areas) means that there is water on the surface.*

Figure 4-6 and Figure 4-7 show the simulated recharge and discharge areas for the regional model simulated using the warm climate with high (Figure 4-6) and low (Figure 4-7) summer precipitation. Both figures show simulated, monthly average data for August in the last year of the model simulation. August was chosen as it is the "driest" month according to the climate data used for in the simulation, i.e. August has the highest average temperature (Figure 3-2), low precipitation (Figure 3-3), and high evapotranspiration (Figure 3-3).

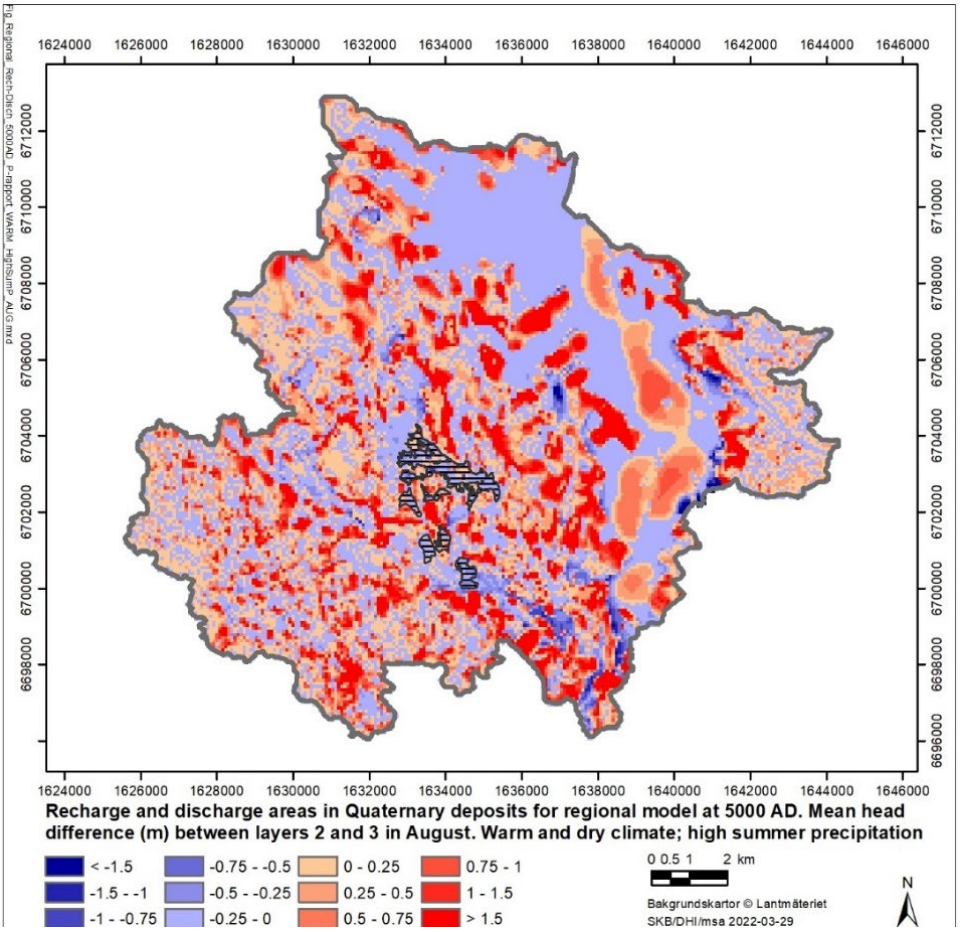


***Figure 4-6.*** *Calculated areas with recharge (red colors) and discharge (blue colors for the regional model run with a warm climate with a high summer precipitation. The map is illustrated for the average in August during the last year of simulation. The darker color the stronger discharge or recharge area.*

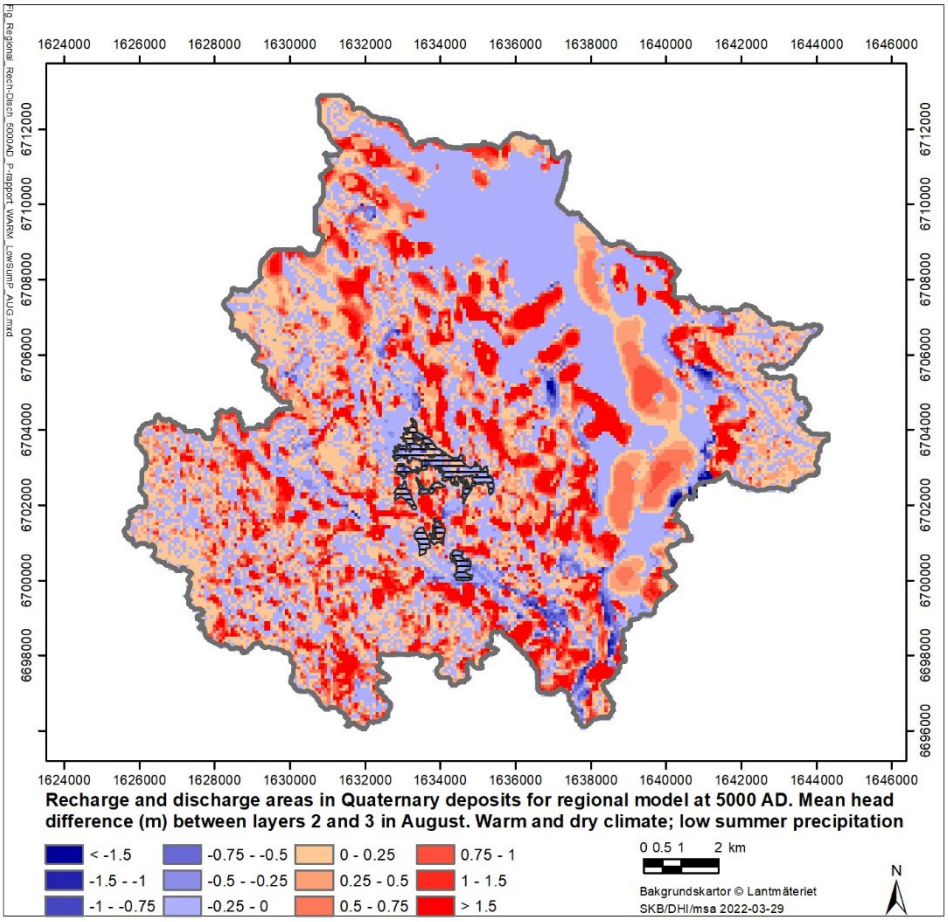


***Figure 4-7.*** *Calculated areas with recharge (red colors) and discharge (blue colors) for the regional model run with a warm climate with a low summer precipitation. The map is illustrated for the average in August during the last year of simulation. The darker color the stronger discharge or recharge area.*

## 4.2 Local model

The time varying boundary conditions for the local model were taken from the results of the regional model. The last five years of each regional model simulations were used as time varying boundary conditions for their respective local model simulations. The last two years of each regional model simulation were then repeated an additional two-times making a total of nine years of simulation time for the local models (5 years + 2 years + 2 years). This was done in order to ensure small changes in annual storages in the later years of the local model simulations. All water balances presented in this section were extracted based on the entire local model area, see Figure 2-3.

### 4.2.1 Warm climate with high summer precipitation

Table 4-3 and Table 4-4 show the annual values for the main water balance components of the local model for the warm climate with high (Table 4-3) and low (Table 4-4) summer precipitation datasets. Results are presented for each of the eight years the models were run. Minor differences in the yearly precipitation used by the model (~1 mm/yr) were observed throughout the simulations due to the adaptive time-stepping procedures used in MIKE SHE. These changes are not presented.

**Table 4-3. Main model water balance items for the local model for each calculated year for the warm climate scenario with high summer precipitation. All numbers are presented in mm/year.**

| Simulation Year | Evapo-transpiration | ΔS Canopy[a] | ΔS Overland[b] | ΔS Sub-surface[c] | Change in net flows to River | Change in net boundary outflow | Error |
|---|---|---|---|---|---|---|---|
| 1 | 543 | 0.00 | 86.3 | -112.4 | - | - | 14.9 |
| 2 | 545 | 0.00 | -0.1 | -11.4 | -6.7 | -25 | -0.3 |
| 3 | 542 | 0.04 | 0.5 | -2.2 | -6.6 | -2.3 | -3.1 |
| 4 | 546 | 0.00 | 0.2 | -2.7 | -0.2 | 0.3 | -0.2 |
| 5 | 546 | 0.00 | 0.1 | -1.9 | -1 | -0.6 | -1.1 |
| 6 | 546 | 0.00 | 0.2 | 0.0 | -0.2 | 0.2 | 1.1 |
| 7 | 546 | 0.00 | 0.1 | -1.4 | 0.3 | -0.2 | -0.5 |
| 8 | 546 | 0.00 | 0.1 | 0.0 | -0.4 | 0.2 | 0.8 |
| 9 | 546 | 0.00 | 0.0 | -1.2 | 0.3 | -0.2 | -0.4 |

[a]: also known as "interception" in the model nomenclature
[b]: "surface" water in rivers and lakes. Also known as "ponded" water in the model nomenclature
[c]: includes water in both the saturated and unsaturated zone

**Table 4-4. Main model water balance items for the local model for each calculated year for the warm climate scenario with low summer precipitation. All numbers are presented in mm/year.**

| Simulation Year | Evapo-transpiration | ΔS Canopy[a] | ΔS Overland[b] | ΔS Sub-surface[c] | Change in net flows to River | Change in net boundary outflow | Error |
|---|---|---|---|---|---|---|---|
| 1 | 537 | 0.00 | 82.11 | -141.18 | - | - | 18.21 |
| 2 | 540 | 0.00 | -0.42 | -21.21 | -30.28 | -30.33 | -3.55 |
| 3 | 539 | 0.04 | 0.13 | -8.14 | -7.38 | -0.56 | -1.37 |
| 4 | 542 | 0.00 | -0.03 | -4.57 | -3.78 | -2.81 | 0.44 |
| 5 | 542 | 0.00 | 0.05 | -3.55 | -1.00 | -0.36 | 0.3 |
| 6 | 541 | 0.00 | 0.05 | -1.68 | -0.60 | -0.25 | 0.32 |
| 7 | 541 | 0.00 | 0.07 | -1.30 | 0.31 | 0.06 | 1.09 |
| 8 | 541 | 0.00 | 0.05 | -1.30 | 2.29 | -0.22 | 0.91 |
| 9 | 540 | 0.00 | 0.08 | -0.41 | -3.24 | 0 | -0.3 |

[a]: also known as "interception" in the model nomenclature
[b]: "surface" water in rivers and lakes. Also known as "ponded" water in the model nomenclature
[c]: includes water in both the saturated and unsaturated zone

For the first year of each simulation the total error is relatively high for both climate scenarios (about 15–18 mm/year) but then decreases to an absolute error of less than 4 mm/year after one year of simulation for both climate scenarios. After three years of simulation, the absolute errors for both climate scenarios remain less than 1.1 mm/year for the remainder of the simulation period.

Figure 4-8 and Figure 4-9 show the change in storage over time for the overland model compartments (upper panels) and the subsurface model compartments (lower panels) for the local model simulated using the warm climate with high (Figure 4-8) and low (Figure 4-9) summer precipitation datasets. Results from both scenarios indicate that the differences in the main water balance items are small the first year of simulation (Table 4-3 and 4-4, Figure 4-8 and 4-9).

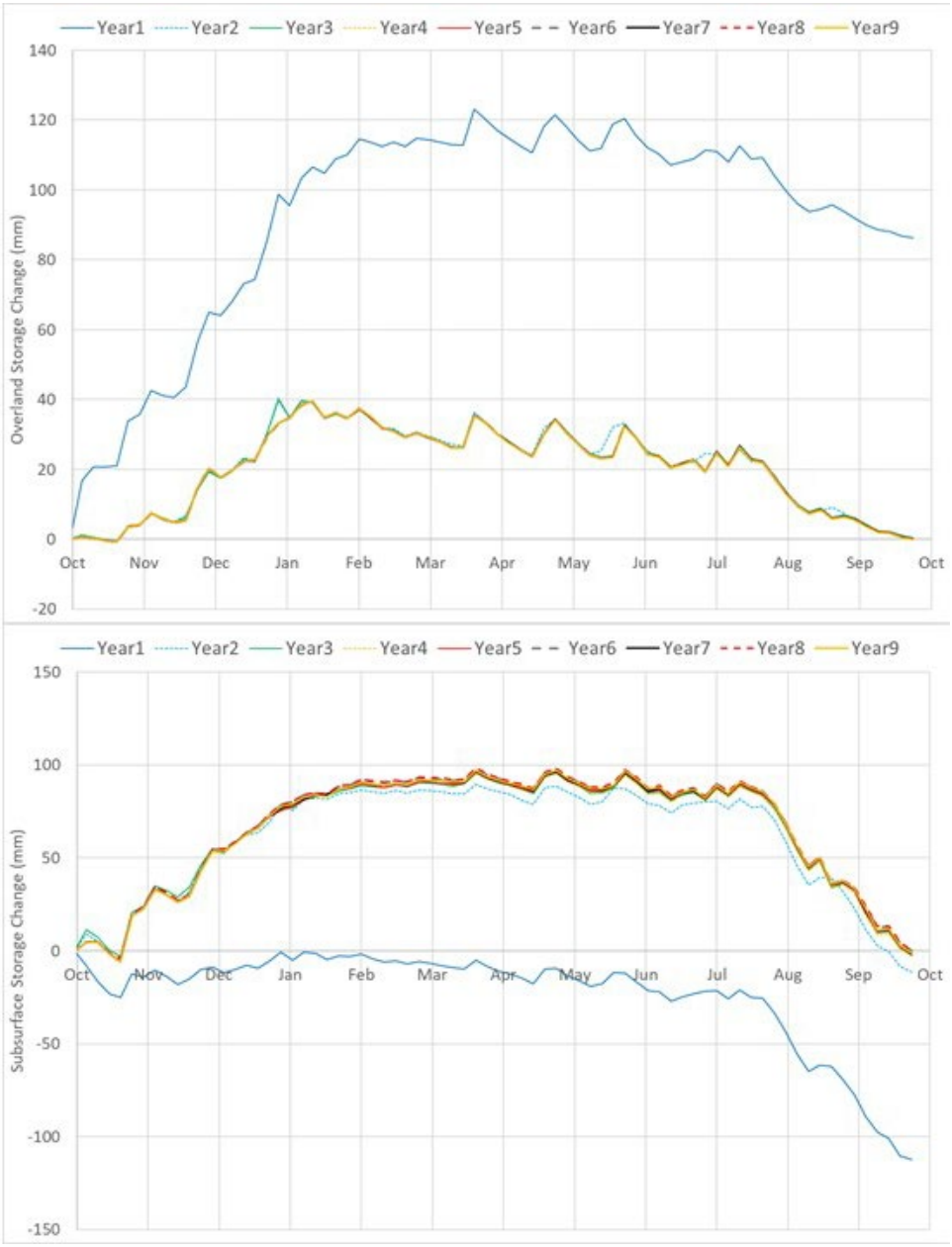


***Figure 4-8.*** *Change of storages in the local model for both surface (upper figure) and subsurface (lower figure) for the warm climate scenario with a high summer precipitation. Each line in the figures represent a year of simulation*

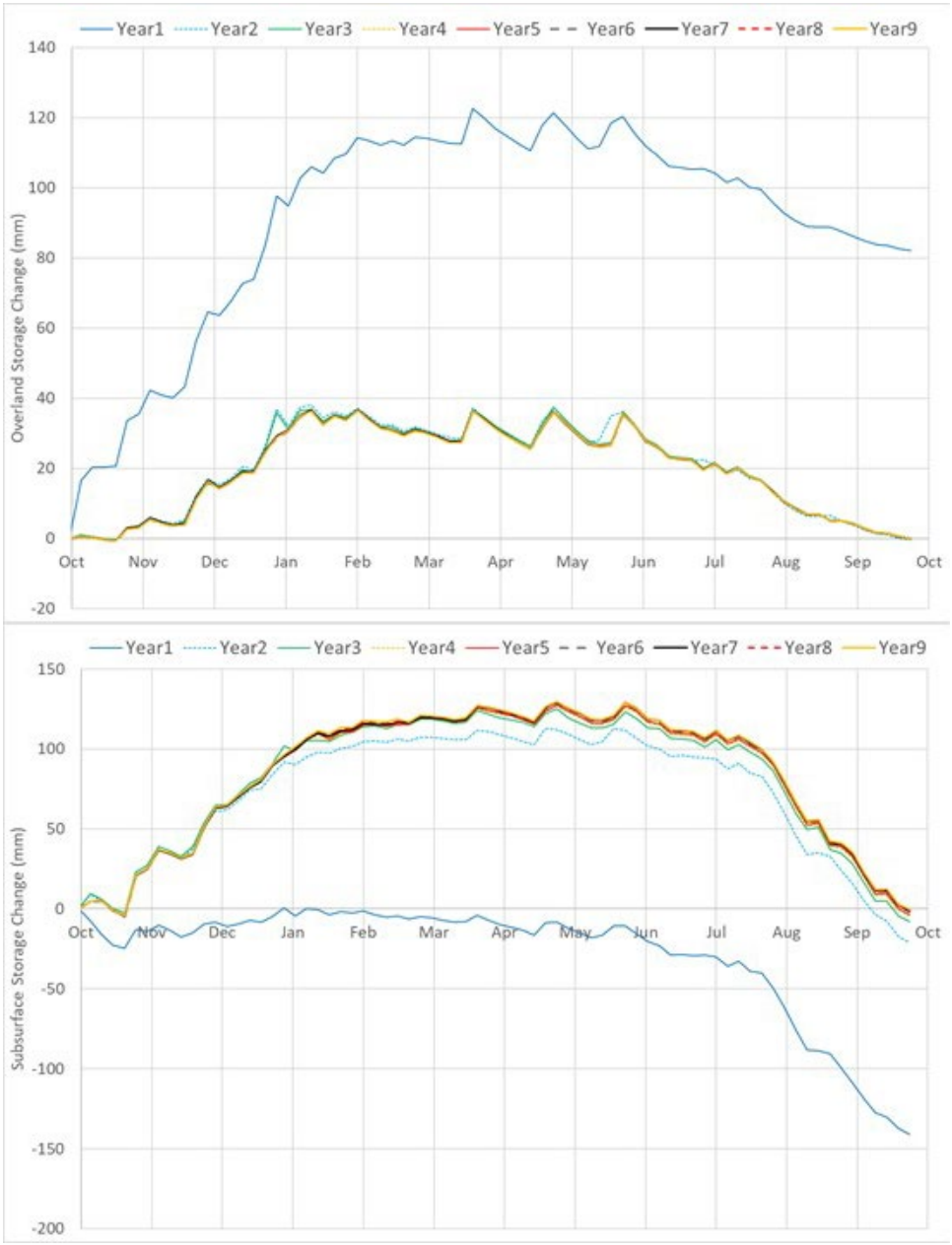


***Figure 4-9.*** *Change of storages in the local model for both surface (upper figure) and subsurface (lower figure) for the warm climate scenario with a low summer precipitation. Each line in the figures represent a year of simulation*

Figure 4-10 and Figure 4-11 show the depth to the phreatic water surface for the local model simulated using the warm climate with high (Figure 4-10) and low (Figure 4-11) summer precipitation datasets. Both figures show simulated, monthly average data for August in the last year of the model simulation. August was chosen as it is the "driest" month according to the climate data used for in the simulation, i.e. August has the highest average temperature (Figure 3-2), low precipitation (Figure 3-3), and high evapotranspiration (Figure 3-3).

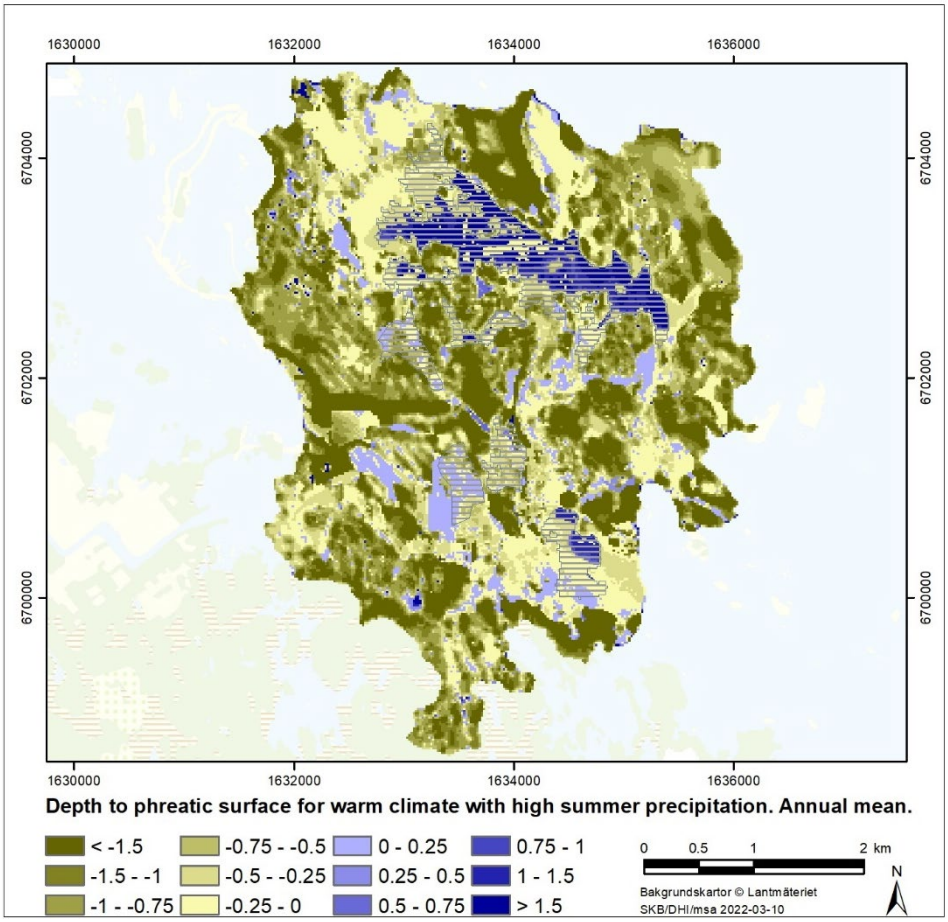


***Figure 4-10.*** *Depth to the phreatic surface for the local model as an annual mean for the last year of calculation for the warm climate with a high summer precipitation. Positive values (blue areas) means that there is water on the surface.*

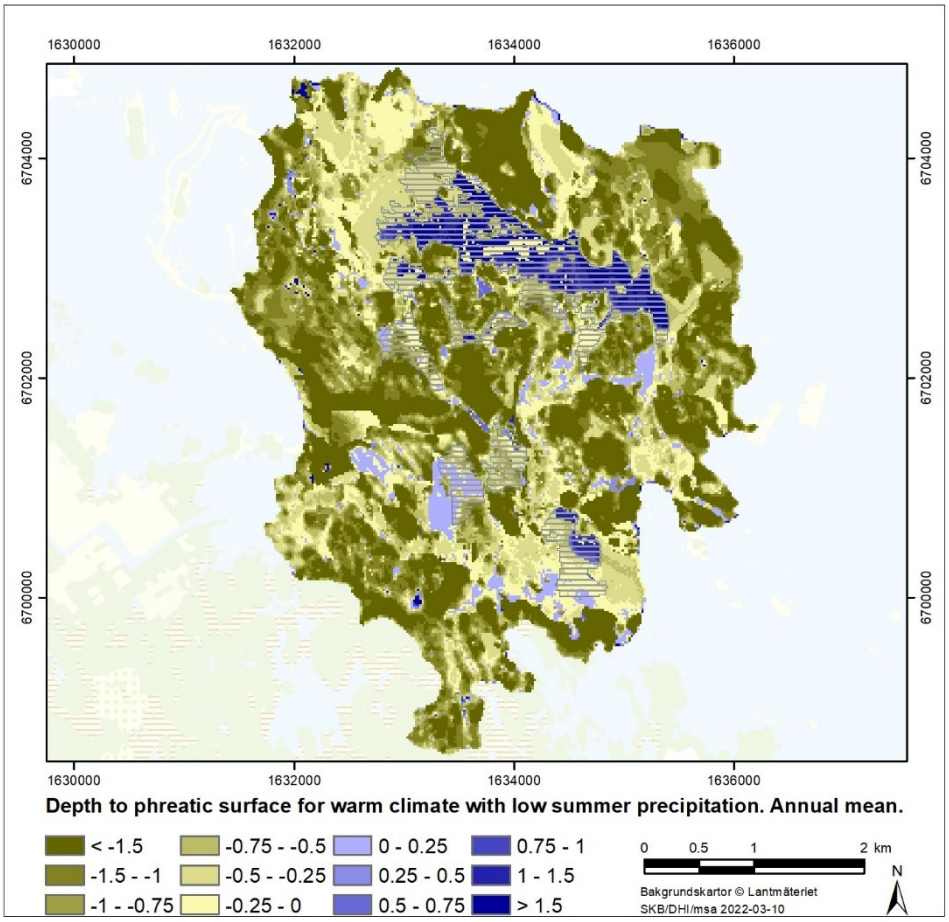


***Figure 4-11.*** *Depth to the phreatic surface for the local model as an annual mean for the last year of calculation for the warm climate with a low summer precipitation. Positive values (blue areas) means that there is water on the surface.*

Figure 4-12 and Figure 4-13 show the simulated recharge and discharge areas for the regional model simulated using the warm climate with high (Figure 4-12) and low (Figure 4-13) summer precipitation. Both figures show simulated, monthly average data for August in the last year of the model simulation. August was chosen as it is the "driest" month according to the climate data used for in the simulation, i.e. August has the highest average temperature (Figure 3-2), low precipitation (Figure 3-3), and high evapotranspiration (Figure 3-3).

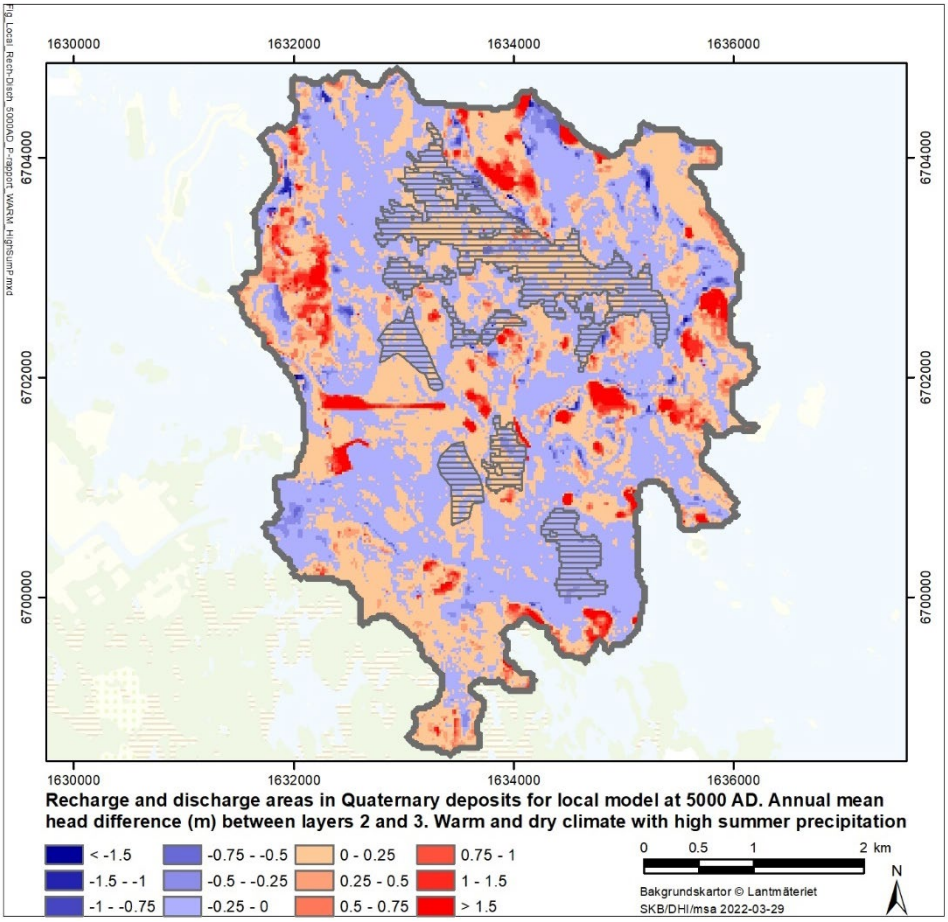


***Figure 4-12.*** *Calculated areas with recharge (red colors) and discharge (blue colors) for the local model run with a warm climate with a high summer precipitation. The map is illustrated for the annual average during the last year of simulation. The darker color the stronger discharge or recharge area.*

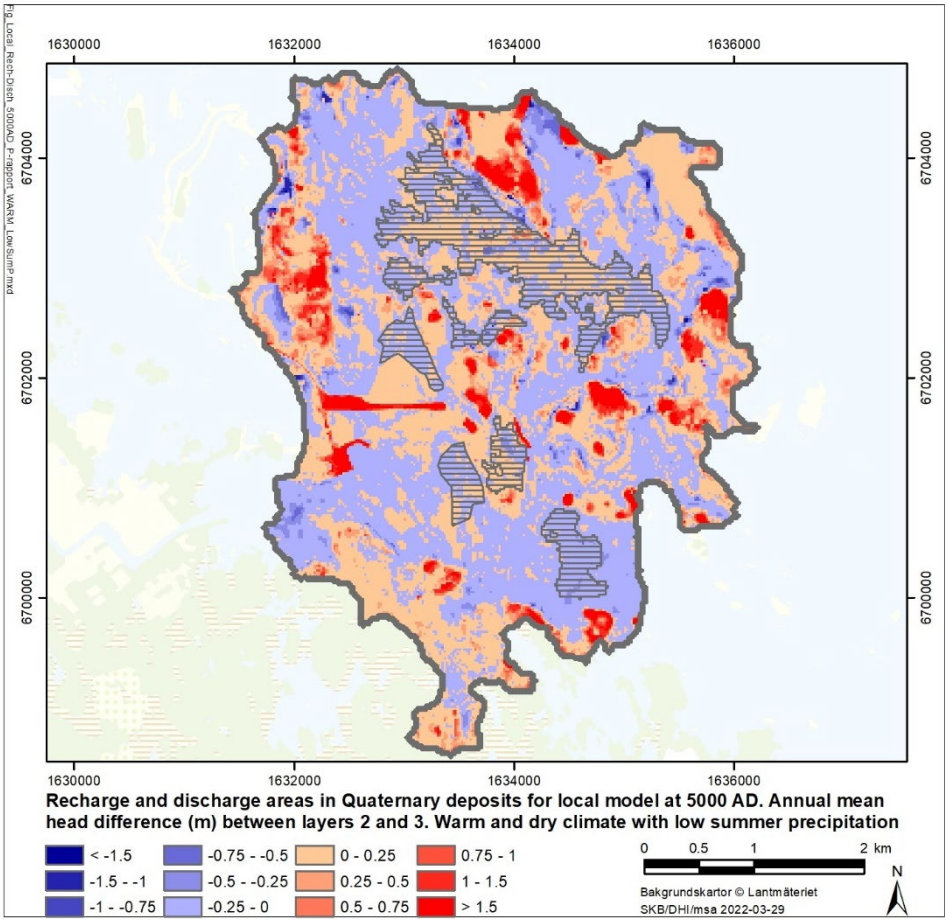


***Figure 4-13.*** *Calculated areas with recharge (red colors) and discharge (blue colors) for the local model run with a warm climate with a low summer precipitation. The map is illustrated for the annual average during the last year of simulation. The darker color the stronger discharge or recharge area.*

Figure 4-14 and Figure 4-15 show the water balances for the local model simulated using the warm climate with high (Figure 4-14) and low (Figure 4-15) summer precipitation. Water balances are calculated using results from the last year of simulation and are considered representative of the typical yearly water balance for the regional model domain according to the respective climate inputs (i.e. high and low summer precipitation climate scenarios).

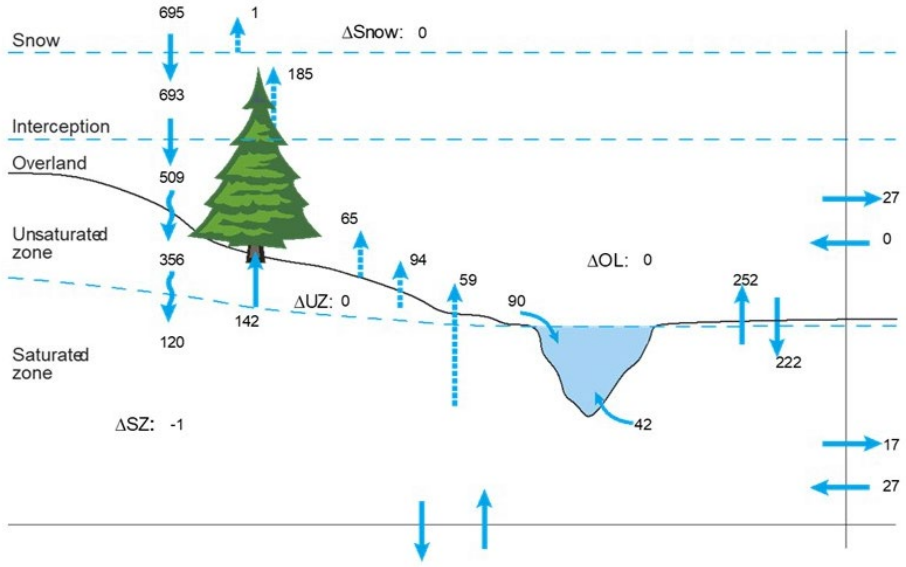


***Figure 4-14.*** *Water balance for the last year of calculation for the local model with the warm climate with high summer precipitation. All numbers are presented in mm. The annual precipitation is 695 mm, the total evapotranspiration is 546 mm and the total runoff is 149 mm.*

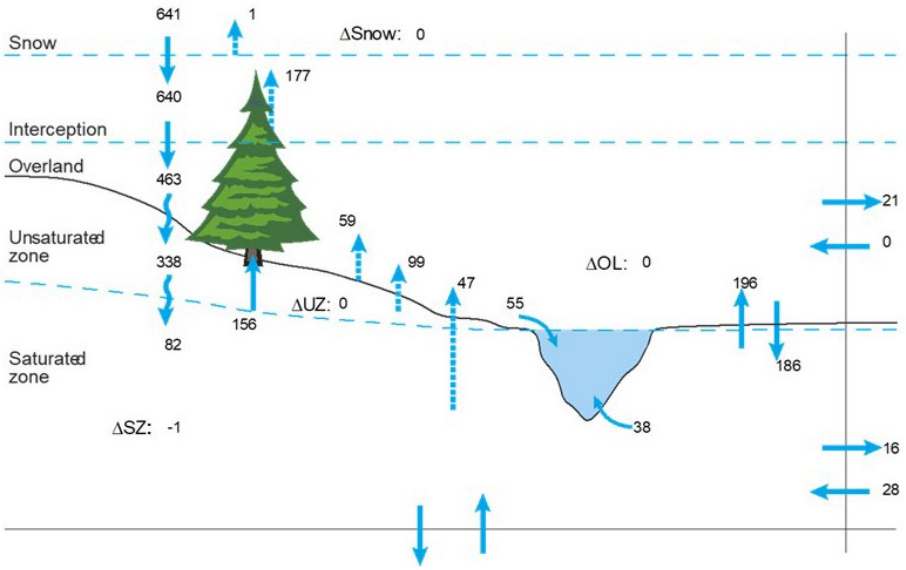


***Figure 4-15.*** *Water balance for the last year of calculation for the local model with the warm climate with low summer precipitation. All numbers are presented in mm. The annual precipitation is 641 mm, the total evapotranspiration is 539 mm and the total runoff is 102 mm.*

# 5 Results for biosphere objects

In the following section, water balances are presented for the four biosphere objects 157_1, 157_2, 159 and 116 (see Figure 2-5). Much like the water balances presented for the local models presented in Figure 4-14 and Figure 4-15 above, the water balances for the biosphere objects are calculated using the MIKE SHE results specific to the spatial delineation of the biosphere objects. Depending on the development phase of the objects (lake, mire, stream) the resulting water balance is presented either according to Figure 2-6 or Figure 2-7.

## 5.1 Biosphere object 157_2

Biosphere object 157_2 is the object examined in this study that is predicted to consist of a mire area without a corresponding stream and/or lake. The surface area of the portion of the model used to extract the water balance for object 157_2 is 167 600 m$^2$.

Figure 5-1 and Figure 5-2 show the water balance results for object 157_2 for the warm climate with high (Figure 5-1) and low summer precipitation (Figure 5-2). All results are presented in mm/year. For the warm climate with high summer precipitation the yearly precipitation is 695 mm, which is 54 mm more that for the year with low summer precipitation. In the water balance results for object 157_2, the net precipitation (precipitation minus all evapotranspiration) is 145 mm for the case with the high summer precipitation (Figure 5-1) compared to 90 mm for the case with low summer precipitation (Figure 5-2). This implies that the modelled evapotranspiration for object 157_2 is similar in the two the climate scenarios. Based on annual water balance values, object 157_2 is considered a discharge area, i.e. there is a net annual discharge of 84 or 95 mm from the bedrock (Figures 5-1 and 5-2). That most of the area in the object is a discharge area can also be seen as net negative pressure difference between the bedrock and bottom regolith layers (Figures 4-12 and 4-13).).

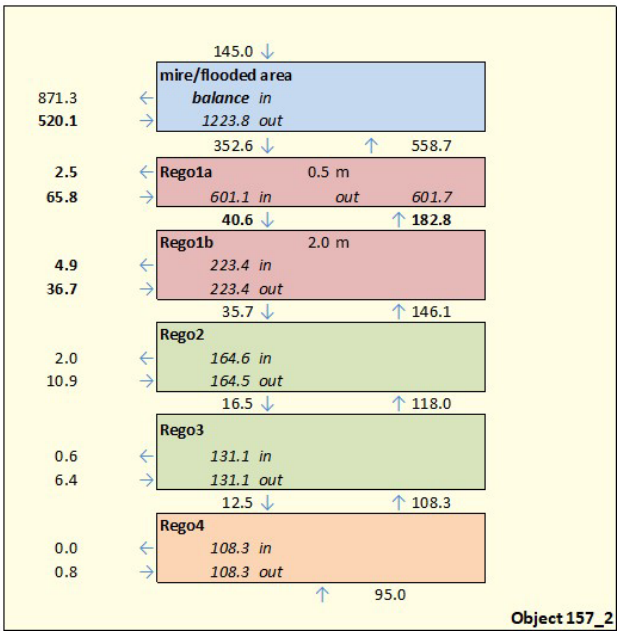


***Figure 5-1.*** *Water balance results for object 157_2 for a warm climate with high summer precipitation. All numbers are given in mm/year.*

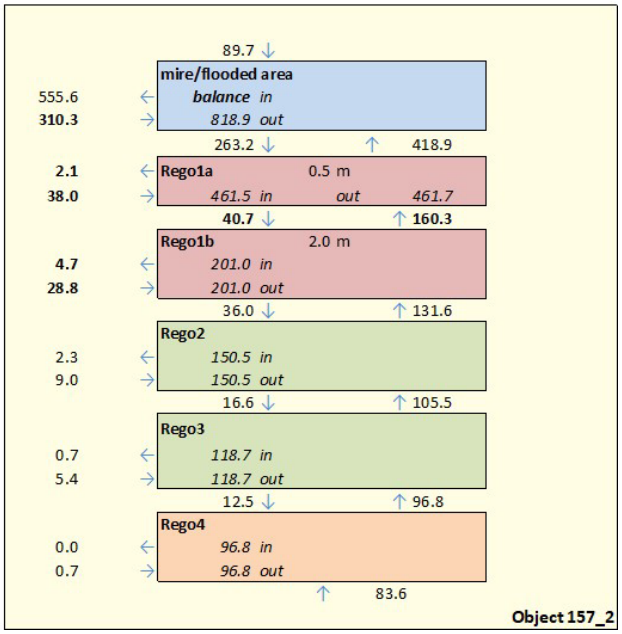


***Figure 5-2.*** *Water balance results for object 157_2 for a warm climate with low summer precipitation. All numbers are given in mm/year.*

## 5.2 Biosphere object 159

Biosphere object 159 is located east of object 157_2 (Figure 2-5). Like object 157_2, there is not an object upstream of object 159. The area of the portion of the model used to extract the water balance surrounding object 159 is the smallest of the four objects in this study with a total area of 103 600 $m^2$; 8400 $m^2$ of the water balance area is predicted to consist of a lake with the remaining area (95 200 $m^2$) predicted to consist of mire.

Figure 5-3 and Figure 5-4 show the water balance results for object 159 for the warm climate with high (Figure 5-3) and low summer precipitation (Figure 5-4). For the mire area, the net precipitation is about 143 mm for the case with high summer precipitation (Figure 5-3). The corresponding net precipitation for the lake area is only about 10 mm because of the relative high evaporation projected to occur from the open water surface. For the climate scenario with a lower summer precipitation (Figure 5-3) the net rainfall from the mire area is 107 mm which is 36 mm less than for the case with a high summer precipitation (Figure 5-4).

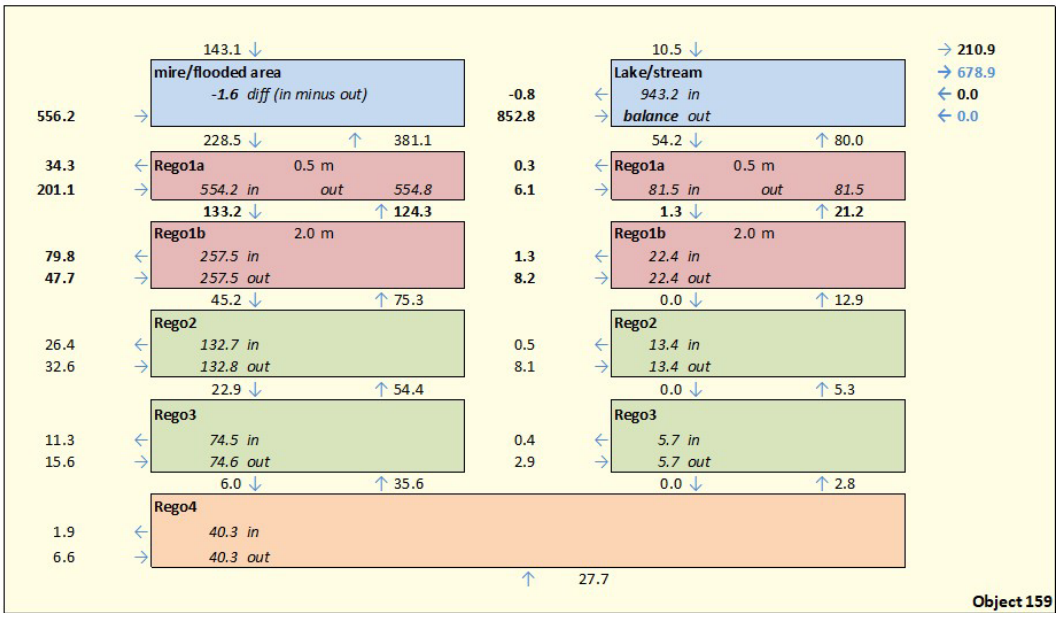


***Figure 5-3.*** *Water balance results for object 159 for a warm climate with high summer precipitation. All numbers are given in mm/year*

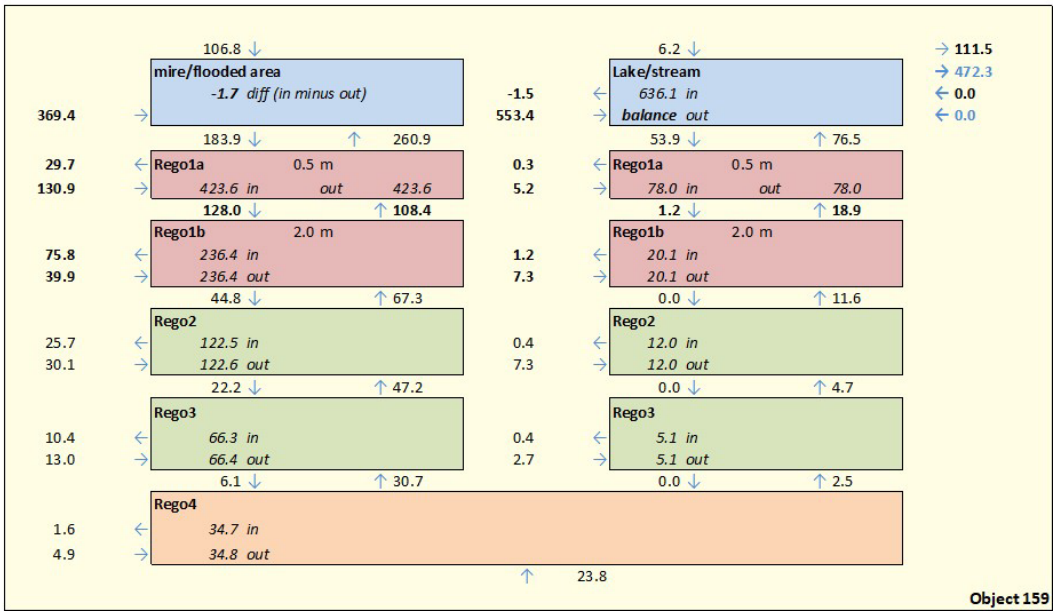


***Figure 5-4.*** *Water balance results for object 159 for a warm climate with low summer precipitation. All numbers are given in mm/year*

## 5.3 Biosphere object 157_1

Biosphere object 157_1 is located downstream of both object 157_2 and 159 (Figure 2-5). The portion of the model used to extract the water balance for object 157_1 has a total area of 105 600 $m^2$; 25 200 $m^2$ of the water balance area is predicted to consist of lake area with the remainder (80 400 $m^2$) predicted to consist of mire.

Figure 5-5 and Figure 5-6 show the water balance results for object 157_1 for the warm climate with high (Figure 5-5) and low summer precipitation (Figure 5-6). For the warm climate with a high summer precipitation, the net precipitation is 102 mm for the mire area and about 31 mm for the lake area (Figure 5-5). Based on annual water balance values, object 157_1 is considered a discharge area (i.e. net negative pressure difference between the bedrock and bottom regolith layers in the MIKE SHE model) but to a lesser extent than objects 157_2 and 159 (Figure 4-12 and Figure 4-13).

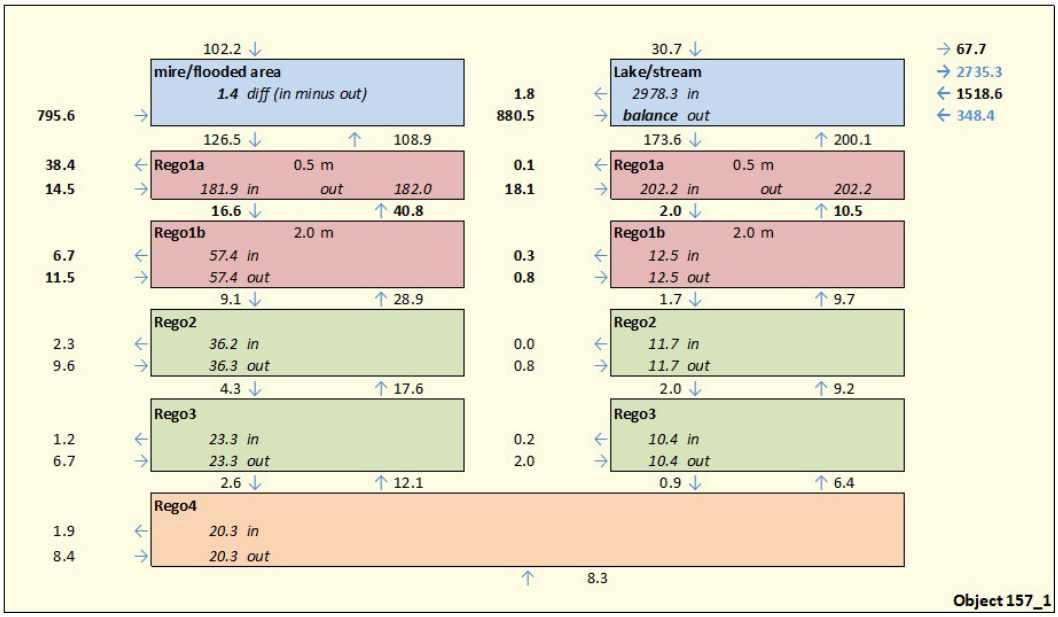


***Figure 5-5.*** *Water balance for biosphere object 157_1 for a warm climate with high summer precipitation. All numbers are given in mm/year.*

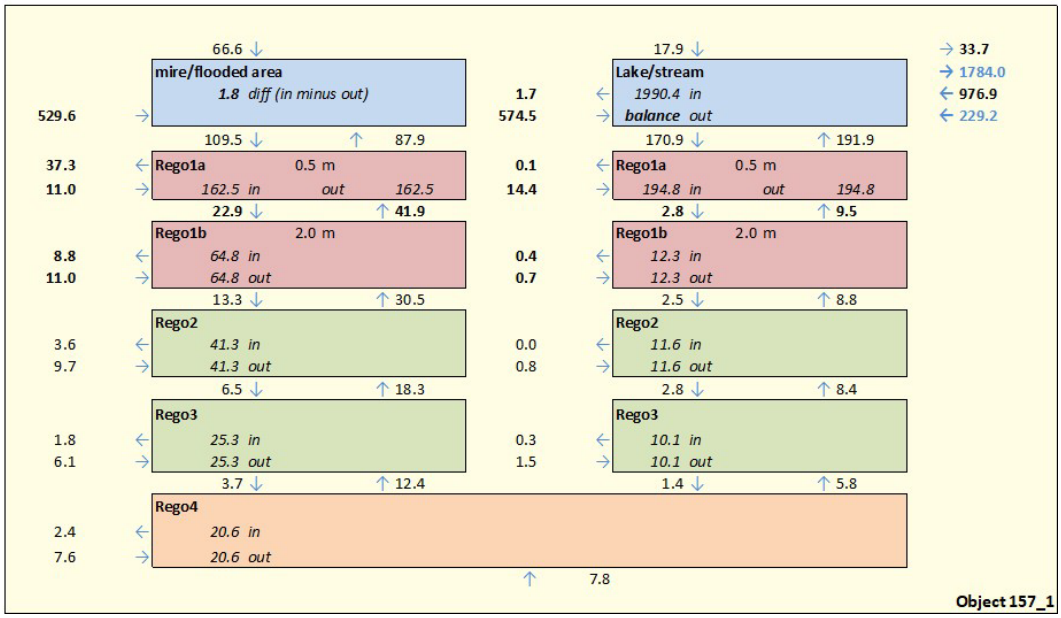


***Figure 5-6.*** *Water balance for biosphere object 157_1 for a warm climate with low summer precipitation. All numbers are given in mm/year.*

## 5.4 Biosphere object 116

The largest object in the present study is object 116. The total water balance area is 1 569 600 $m^2$, of which the lake area is 902 400 $m^2$. Object 116 is located downstream of the three previously presented objects, and also receives water flow from object 158 (see Figure 2-5), which however is not presented in this report.

Figure 5-7 and Figure 5-8 show the water balance results for object 157_1 for the warm climate with high (Figure 5-7) and low summer precipitation (Figure 5-8).

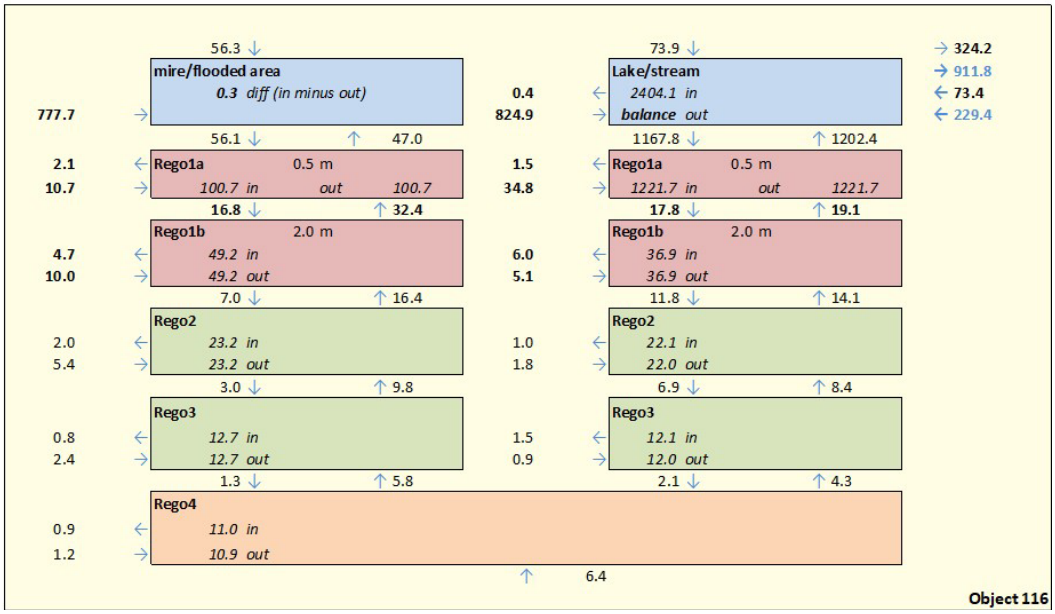


***Figure 5-7.*** *Water balance results for object 116 for a warm climate with high summer precipitation. All numbers are given in mm/year*

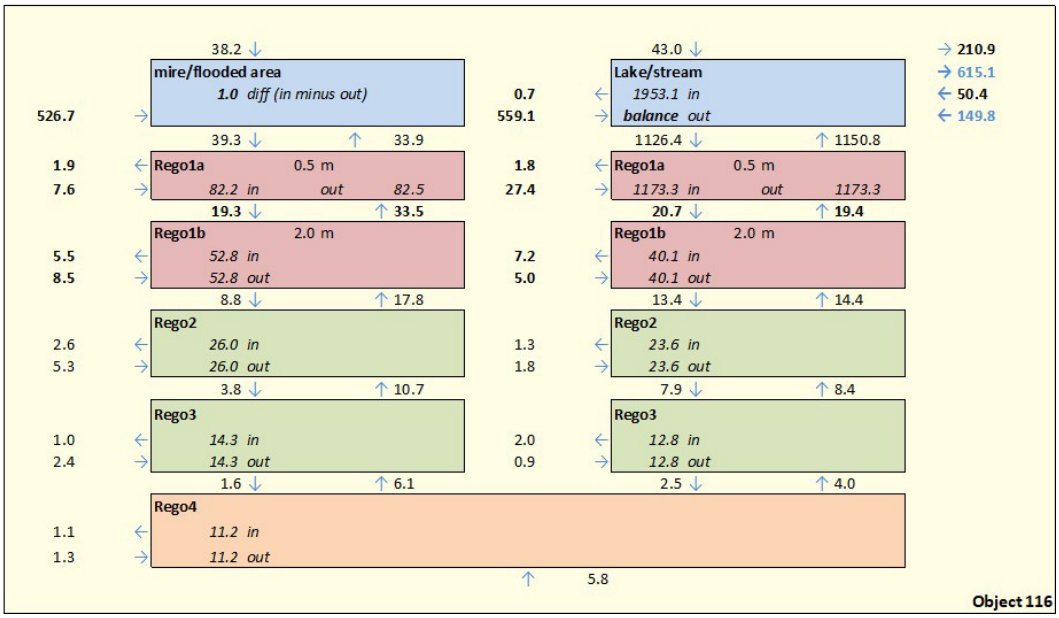


***Figure 5-8.*** *Water balance results for object 116 for a warm climate with low summer precipitation. All numbers are given in mm/year*

# References

SKB's (Svensk Kärnbränslehantering AB) publications can be found at www.skb.com/publications. SKBdoc documents will be submitted upon request to document@skb.se.


**Berger A, 1978.** Long-term variations of daily insolation and Quaternary climatic changes. Journal of the Atmospheric Sciences 35, 2362–2367.

**Berglund S, Bosson E, Sassner M, 2013.** From site data to safety assessment: analysis of present and future hyrological conditions at a coastal site in Sweden. AMBIO 42, 425–434.

**Bosson E, Gustafsson L-G, Sassner M, 2008.** Numerical modelling of surface hydrology and near-surface hydrogeology at Forsmark. Site descriptive modelling, SDM-Site Forsmark. SKB R-08-09, Svensk Kärnbränslehantering AB.

**Bosson E, Sabel U, Gustafsson L-G, Sassner M, Destouni G, 2012.** Influences of shifts in climate, landscape, and permafrost on terrestrial hydrology. Journal of Geophysical Research 117, D05120. doi:10.1029/2011JD016429

**Brydsten L, Strömgren M, 2010.** A coupled regolith-lake development model applied to the Forsmark site. SKB TR-10-56, Svensk Kärnbränslehantering AB.

**Brydsten L, Strömgren M, 2013.** Landscape development in the Forsmark area from the past into the future (8500 BC – 40000 AD). SKB R-13-27, Svensk Kärnbränslehantering AB.

**DHI, 2020.** MIKE SHE – An integrated hydrological modelling system: User's guide. Horsholm, Denmark: DHI.

**Graham D N, Butts M B, 2005.** Flexible, integrated watershed modelling with MIKE SHE. In Singh V P, Frevert D K (eds). Watershed models. Boca Raton, FL: CRC Press, 245–272.

**IPCC, 2013.** Climate change 2013: the physical science basis: summary for policymakers. Contribution of Working Group I to the Fifth Assessment Report of the Intergovernmental Panel on Climate Change. Cambridge: Cambridge University Press.

**Jutebring Sterte E, Johansson E, Sjöberg Y, Huseby Karlsen R, Laudon H, 2018.** Groundwater–surface water interactions across scales in a boreal landscape investigated using a numerical modelling approach. Journal of Hydrology 560, 184–201.

**Jutebring Sterte E, Lidman F, Lindborg E, Sjöberg Y, Laudon H, 2021.** How catchment characteristics influence hydrological pathways and travel times in a boreal landscape. Hydrology and Earth System Sciences 25, 2133–2158.

**Pereira A R, Pruitt W O, 2004.** Adaptation of the Thornthwaite scheme for estimating daily reference evapotranspiration. Agricultural Water Management 66, 251–257.

**Roderick M L, 1992.** Methods for calculating solar position and day length including computer programs and subroutines. Report 137, Department of Agriculture and Food, Western Australia, Perth.

**Sassner M, 2022.** Framtagande av vattenbalanser från MIKE SHE till radionuklidtransportmodellering. Genomgång av metod utvecklad och beskriven i R-13-19. SKBdoc 1987268 ver 1.0. Svensk Kärnbränslehantering AB. (In Swedish)

**SKB TR-23-01.** SKB 2022. Post-closure safety for SFR, the final repository for short-lived radioactive waste at Forsmark. Post-closure safety report, PSAR version. Svensk Kärnbränslehantering AB.

**SKB TR-23-05.** SKB 2022. Post-closure safety for SFR, the final repository for short-lived radioactive waste at Forsmark. Climate and climate-related issues, PSAR version. Svensk Kärnbränslehantering AB.

**Thornthwaite C W, 1948.** An approach toward a rational classification of climate. Geographical Review 38, 55–94.

**Werner K, Sassner M, Johansson E, 2013.** Hydrology and near-surface hydrogeology at Forsmark – synthesis for the SR-PSU project. SR-PSU Biosphere. SKB R-13-19, Svensk Kärnbränslehantering AB.

**Willmott C J, Rowe C M, Mintz Y, 1985.** Climatology of the terrestrial seasonal water cycle. Journal of Climatology 5, 589–606.